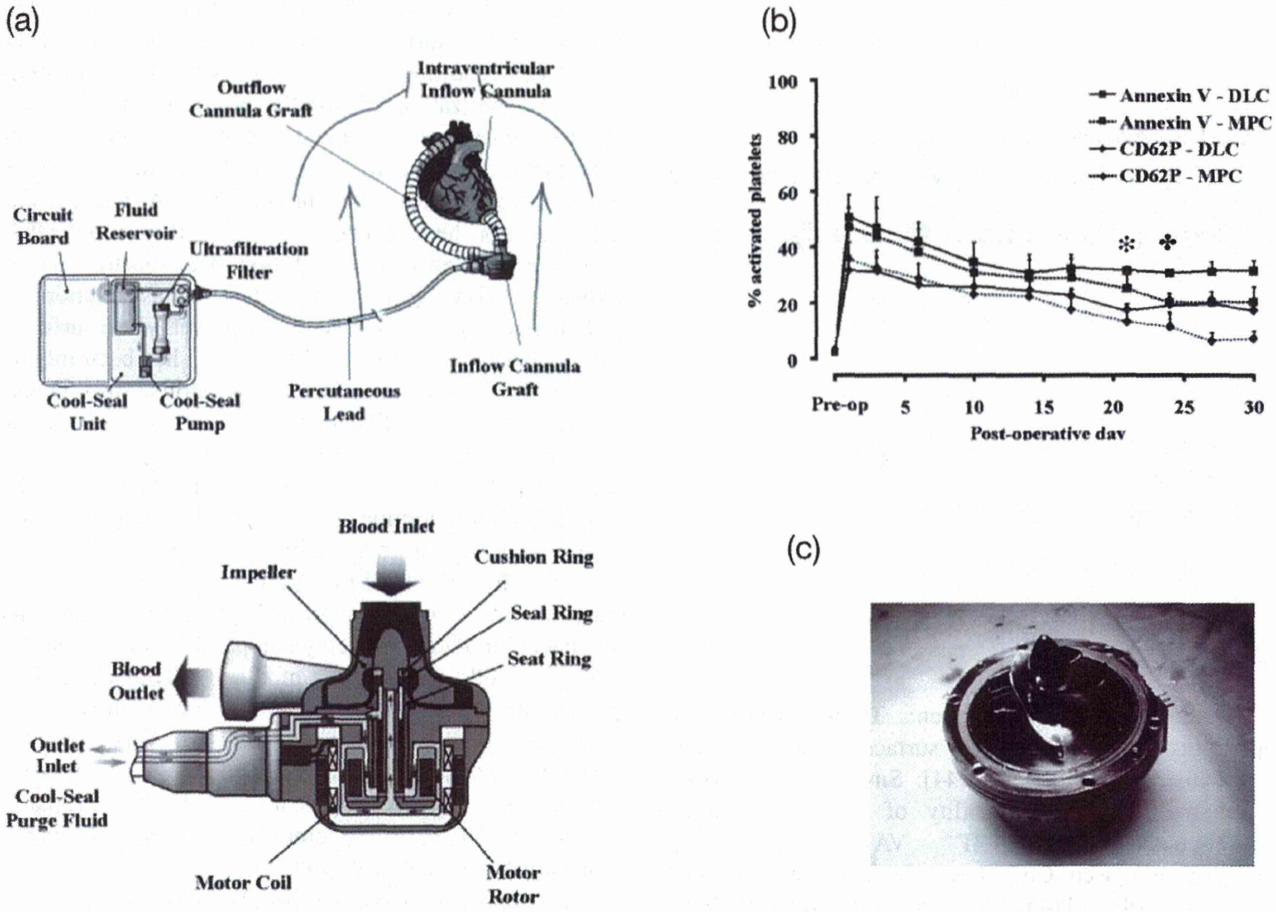

Figure 14. (a) EVAHEART VAD in the preferred anatomic placement for left ventricular support. The system consists of the inflow cannula, pump, outflow cannula, and lubricating purge system. The Cool-Seal purge system consists of a pump, ultrafiltration filter, and reservoir contained in a small case that can be carried by the patient. Water is recirculated through the system by the Cool-Seal pump, the ultrafiltration unit ensures sterility of fluid egressing the unit to the blood pump, and the reservoir can be exchanged or refilled as needed. (b) The concentrations of circulating activated platelets as quantified by annexin V binding or CD62P expression are shown for DLC-coated ($N = 4$) and MPC polymer-coated ($N = 16$) components. The days when the MPC values become significantly lower than the DLC values for annexin V (❊) and CD62P (✤) are marked above the curves. (c) Pump (MPC polymer coating) after 34 days of support without anticoagulation treatment. (Reprinted from [146, 147] with permission from Wiley.)

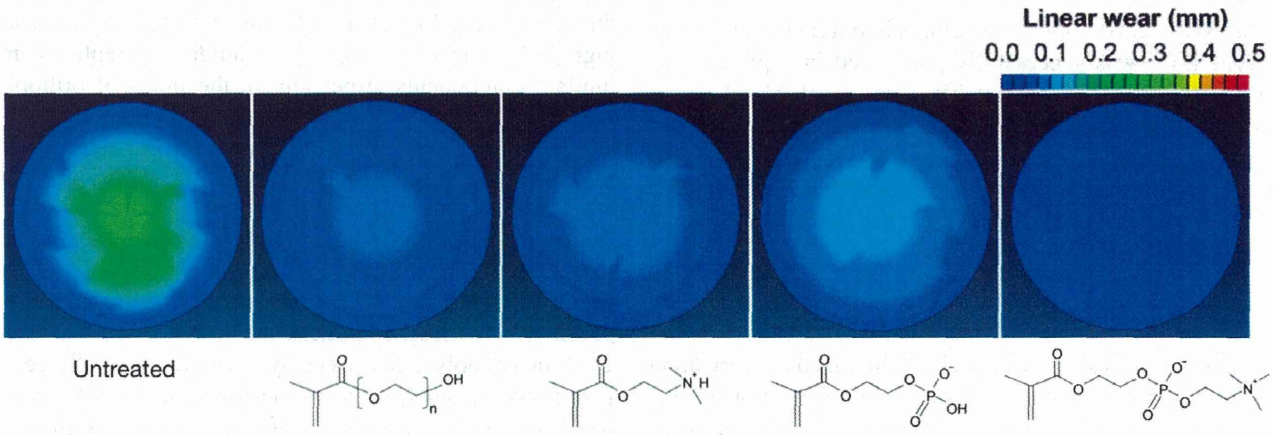

Figure 15. Spatial maps of wear in CLPE cups grafted with poly(MPC) or other polyelectrolytes after a hip simulator test.

hydrogels are normally prepared by copolymerization of macromonomers bearing silicone and hydrophilic monomers. The wettability of the silicone hydrogels is sometimes not adequate to provide the wearer with a comfortable feeling. MPC polymers have been developed for coatings to improve the surface wettability of silicone hydrogels; the surfaces also show good antifouling properties. Through the formation of interpenetrating poly(MPC) networks, Ishihara

and co-workers have succeeded in preparing superhydrophilic silicone hydrogels with a high degree of transparency [52].

5. Conclusions

In this review article, the molecular design and fundamental properties of cell membrane-inspired phospholipid polymers, MPC polymers, are summarized. In addition, surface modification processes using MPC polymers to regulate biological responses are described. MPC polymers are suitable for preparing not only nonfouling surfaces but also platforms of biomolecules and living cells. Through the combination of nanotechnology and biotechnology, MPC polymer science has made considerable progress with devices such as biosensors, biochips and bioimaging tools [154]. MPC and various kinds of MPC polymers are now available commercially worldwide, and many medical devices treated with MPC polymers are used in clinics. Therefore, we expect that the novel biomedical technology based on MPC polymer science will be further explored.

References

[1] Singer S J and Nicolson G L 1972 *Science* **175** 723
[2] Virtanen J A, Cheng K H and Somerharju P 1998 *Proc. Natl Acad. Sci. USA* **95** 4964
[3] Kadoma Y, Nakabayashi N, Masuhara E and Yamauchi J 1978 *Koubunshi Ronbunshu* **35** 423 (in Japanese)
[4] Ishihara K, Ueda T and Nakabayashi N 1990 *Polym. J.* **22** 355
[5] Ueda T, Oshida H, Kurita K, Ishihara K and Nakabayashi N 1992 *Polym. J.* **24** 1259
[6] Inoue Y, Watanabe J, Takai M and Ishihara K 2004 *J. Biomater. Sci. Polym. Edn.* **15** 1153
[7] Ma Y, Tang Y, Billingham N C, Armes S P, Lewis A L, Lloyd A W and Salvage J P 2003 *Macromolecules* **36** 3475
[8] Ma Y, Tang Y, Billingham N C, Armes S P and Lewis A L 2003 *Biomacromolecules* **4** 864
[9] Li Y, Armes S P, Jin X and Zhu S 2003 *Macromolecules* **36** 8268
[10] Ishihara K, Tsuji T, Kurosaki K and Nakabayashi N 1994 *J. Biomed. Mater. Res.* **28** 225
[11] Iwasaki Y and Akiyoshi K 2004 *Macromolecules* **37** 7637
[12] Watanabe J, Eriguchi T and Ishihara K 2002 *Biomacromolecules* **3** 1109
[13] Watanabe J, Eriguchi T and Ishihara K 2002 *Biomacromolecules* **3** 1375
[14] Samanta D, McRae S, Cooper B, Hu Y, Emrick T, Pratt J and Charles S A 2008 *Biomacromolecules* **9** 2891
[15] Ishihara K 2012 *Encyclopedia Polym. Sci. Tech.* at press
[16] Kiritoshi Y and Ishihara K 2004 *Polymer* **45** 7499
[17] Lobb E J, Ma I, Billingham N C, Armes S P and Lewis A L 2001 *J. Am. Chem. Soc.* **123** 791
[18] Ma I, Lobb E J, Billingham N C, Armes S P, Lewis A L, Lloyd A W and Salvage J 2002 *Macromolecules* **35** 9306
[19] Madsen J, Warren N J, Armes S P and Lewis A L 2011 *Biomacromolecules* **12** 2225
[20] Seo J H, Matsuno R, Lee Y, Takai M and Ishihara K 2009 *Biomaterials* **30** 4859
[21] Chen X, McRae S, Samanta D and Emrick T 2010 *Macromolecules* **43** 6261
[22] Xu J P, Ji J, Chen W D and Shen J C 2005 *Macromol. Biosci.* **5** 164
[23] Iwasaki Y and Akiyoshi K 2006 *Biomacromolecules* **7** 1433
[24] Li Y, Tang Y, Narain R, Lewis A L and Armes S P 2005 *Langmuir* **21** 9946
[25] Yusa S, Fukuda K, Yamamoto T, Ishihara K and Morishima Y 2005 *Biomacromolecules* **6** 663
[26] Bhuchar N, Thundat T, Sunasee R, Ishihara K and Narain R 2012 *Bioconjug. Chem.* **23** 75
[27] Bhuchar N, Deng Z, Ishihara K and Narain R 2011 *Polym. Chem.* **2** 623
[28] Yu B, Lowe A B and Ishihara K 2009 *Biomacromolecules* **10** 950
[29] Yuan J J, Schmid A, Armes S P and Lewis A L 2006 *Langmuir* **22** 11022
[30] Akkahat P, Kiatkamjornwong S, Yusa S, Hoven V P and Iwasaki Y 2012 *Langmuir* **28** 5872
[31] Iwasaki Y, Matsumoto A and Yusa S 2012 *ACS Appl. Mater. Interfaces* **4** 3254
[32] Iwasaki Y and Ishihara K 2005 *Anal. Bioanal. Chem.* **381** 534
[33] Ishihara K, Oshida H, Endo Y, Ueda T, Watanabe A and Nakabayashi N 1992 *J. Biomed. Mater. Res.* **26** 1543
[34] Ishihara K, Iwasaki Y and Nakabayashi N 1999 *Polym. J.* **31** 1231
[35] Yamasaki A, Imamura Y, Kurita K, Iwasaki Y, Nakabayashi N and Ishihara K 2003 *Colloid. Surf.* B **28** 53
[36] Iwasaki Y, Yamasaki A and Ishihara K 2003 *Biomaterials* **24** 3599
[37] Lewis A L, Hughes P D, Kirkwood L C, Leppard S W, Redman R P, Tolhurst L A and Stratford P W 2000 *Biomaterials* **21** 1847
[38] Futamura K, Matsuno R, Konno T, Takai M and Ishihara K 2008 *Langmuir* **24** 10340
[39] Fukazawa K and Ishihara K 2012 *Colloid. Surf.* B **97** 70
[40] Iwasaki Y, Takamiya M, Iwata R, Yusa S and Akiyoshi K 2007 *Colloid. Surf.* B **57** 226
[41] Choi J, Konno T, Takai M and Ishihara K 2012 *Biomaterials* **33** 954
[42] Choi J, Konno T, Matsuno R, Takai M and Ishihara K 2008 *Colloid. Surf.* B **67** 216
[43] Pang S, Zhu C, Xu F, Chen C and Ji J 2012 *Colloid. Surf.* B **94** 22
[44] Ishihara K, Hanyuda H and Nakabayashi N 1995 *Biomaterials* **16** 873
[45] Ishihara K, Shibata N, Tanaka S, Iwasaki Y, Kurosaki T and Nakabayashi N 1996 *J. Biomed. Mater. Res.* **32** 401
[46] Yoneyama T, Ishihara K, Nakabayashi N, Ito M and Mishima Y 1998 *J. Biomed. Mater. Res.* **43** 15
[47] Ishihara K, Fukumoto K, Iwasaki Y and Nakabayashi N 1999 *Biomaterials* **20** 1545
[48] Hasegawa T, Iwasaki Y and Ishihara K 2001 *Biomaterials* **22** 243
[49] Ishihara K, Nishiuchi D, Watanabe J and Iwasaki Y 2004 *Biomaterials* **25** 71
[50] Iwasaki Y, Aiba Y, Morimoto N, Nakabayashi N and Ishihara K 2000 *J. Biomed. Mater. Res.* **52** 701
[51] Morimoto N, Iwasaki Y, Nakabayashi N and Ishihara K 2002 *Biomaterials* **23** 4881
[52] Shimizu T, Goda T, Minoura N, Takai M and Ishihara K 2010 *Biomaterials* **31** 3274
[53] Hoshi T, Sawaguchi T, Matsuno R, Konno T, Takai M and Ishihara K 2012 *J. Mater. Chem.* **20** 4897
[54] Hoshi T, Sawaguchi T, Matsuno R, Konno T, Takai M and Ishihara K 2008 *J. Supercritical Fluids* **44** 391
[55] Ishihara K, Fukumoto K, Aoki J and Nakabayashi N 1992 *Biomaterials* **13** 145
[56] Ishihara K, Miyazaki H, Kurosaki T and Nakabayashi N 1995 *J. Biomed. Mater. Res.* **29** 181
[57] Hsiue G H, Lee S D, Chang P C T and Kao C Y 1998 *J. Biomed. Mater. Res.* **42** 134
[58] Iwasaki Y, Sawada S, Nakabayashi N, Khang G, Lee H B and Ishihara K 1999 *Biomaterials* **20** 2185

[59] Ishihara K, Iwasaki Y, Ebihara S, Shindo Y and Nakabayashi N 2000 *Colloid. Surf.* B **18** 325
[60] Kyomoto M and Ishihara K 2009 *ACS Appl. Mater. Interf.* **1** 537
[61] Feng W, Brash J and Zhu S P 2004 *J. Polym. Sci. A: Polym. Chem.* **42** 2931
[62] Iwata R, Suk-In P, Hoven V P, Takahara A, Akiyoshi K and Iwasaki Y 2004 *Biomacromolecules* **5** 2308
[63] Feng W, Zhu S, Ishihara K and Brash J L 2005 *Langmuir* **21** 5980
[64] Tsujii Y, Ohno K, Yamamoto S Goto A and Fukuda T 2006 *Adv. Polym. Sci.* **197** 1
[65] Ishihara K, Nomura H, Mihara T, Kurita K, Iwasaki Y and Nakabayashi N 1998 *J. Biomed. Mater. Res.* **39** 323
[66] Konno K, Watanabe J and Ishihara K 2004 *Biomacromolecules* **5** 342
[67] Kinoshita K *et al* 2006 *Nucleic Acids Res.* **35** e3
[68] Iwata R, Sato R, Iwasaki Y and Akiyoshi K 2008 *Colloid. Surf.* B **62** 288
[69] Chantasirichot S and Ishihara K 2012 *Biosens. Bioelectron.* **38** 209
[70] Watanabe J and Ishihara K 2006 *Biomacromolecules* **7** 171
[71] Watanabe J and Ishihara K 2007 *Nanobiotechnology* **3** 76
[72] Goto Y, Matsuno R, Konno T, Takai M and Ishihara K 2008 *Biomacromolecules* **9** 3252
[73] Ishihara K, Goto Y, Matsuno R, Inoue Y and Konno T 2012 *Biochim. Biophys. Acta* **1810** 268
[74] Matsuno R and Ishihara K 2011 *Nano Today* **6** 61
[75] Ishihara K, Aragaki R, Ueda T, Watanabe A and Nakabayashi N 1990 *J. Biomed. Mater. Res.* **24** 1069
[76] Ishihara K, Ziats N P, Tierney B P, Nakabayashi N and Anderson J M 1991 *J. Biomed. Mater. Res.* **25** 1397
[77] Ishihara K, Oshida H, Endo Y, Watanabe A, Ueda T and Nakabayashi N 1993 *J. Biomed. Mater. Res.* **27** 1309
[78] Zhang S, Benmakroha, Rolf P, Tanaka S and Ishihara K 1996 *Biosens. Bioelectron.* **11** 1019
[79] Fujii K, Matsumoto H N, Koyama Y, Iwasaki Y, Ishihara K and Takakuda K 2008 *J. Vet. Med. Sci.* **70** 167
[80] Nakai K, Morigaki K and Iwasaki Y 2010 *Soft Matter* **6** 5937
[81] Iwasaki Y, Mikami A, Kurita K, Ishihara K and Nakabayashi N 1997 *J. Biomed. Mater. Res.* **36** 508
[82] Matyjaszewski K and Xia J 2001 *Chem. Rev.* **101** 2921
[83] Matyjaszewski K *et al* 1999 *Macromolecules* **32** 8716
[84] Kong X, Kawai T, Abe J and Iyoda T 2001 *Macromolecules* **34** 1837
[85] Huang W, Kim J B, Bruening M L and Baker G L 2002 *Macromolecules* **35** 1175
[86] Shah R R, Merreceyes D, Husemann M, Rees I, Abbott N L, Hawker C J and Hedrick J L 2000 *Macromolecules* **33** 597
[87] Jones D M and Huck W T S 2001 *Adv. Mater.* **13** 1256
[88] Tsujii Y, Ejaz M, Yamamoto S, Fukuda T, Shigeto K, Mibu K and Shinjo T 2002 *Polymer* **43** 3837
[89] Maeng I S and Park J W 2003 *Langmuir* **19** 9973
[90] Inoue Y, Nakanishi T and Ishihara K 2011 *React. Funct. Polym.* **71** 350
[91] Feng W, Brash J L and Zhu S 2006 *Biomaterials* **27** 847
[92] Yoshimoto K, Hirase T, Madsen J, Armes S P and Nagasaki Y 2009 *Macromol. Rapid. Commun.* **30** 2136
[93] Kobayashi M, Yamaguchi H, Terayama Y, Wang Z, Ishihara K, Hino M and Takahara A 2009 *Macromol. Symp.* **279** 79
[94] Kobayashi M and Takahara A 2010 *Chem. Rec.* **10** 208
[95] Iwasaki Y, Sawada S, Ishihara K, Khang G and Lee H B 2002 *Biomaterials* **23** 3897
[96] Sawada S, Sakaki S, Iwasaki Y, Nakabayashi N and Ishihara K 2003 *J. Biomed. Mater. Res.* A **64** 411
[97] Pricer W E, Hudgin R L, Ashwell G, Stockert R J and Morell A G 1974 *Methods Enzymol.* **34** 688
[98] Stockert R J 1995 *Physiol. Rev.* **75** 591
[99] Weigel P H, Scnnaar R L, Kuhlenschmidt M S, Schmell E, Lee R T, Lee Y C and Roseman S 1979 *J. Biol. Chem.* **254** 10830
[100] Kobayashi A, Akaike T, Kobayashi K and Sumitomo H 1986 *Makromol. Chem., Rapid Commun.* **7** 645
[101] Gutsche A T, Parsons-Wingerter P, Chand D, Saltzman W M and Leong K W 1994 *Biotechnol. Bioeng.* **43** 801
[102] Sagara K and Kim S W 2002 *J. Control. Release* **79** 271
[103] Kim S H, Hoshiba T and Akaike T 2004 *Biomaterials* **25** 1813
[104] Sato K, Miura Y, Saito N, Kobayashi K and Takai O 2007 *Biomacromolecules* **8** 753
[105] Yarema K J, Mahal L K, Bruehl R E, Rodriguez E C and Bertozzi C R 1998 *J. Biol. Chem.* **273** 31168
[106] Iwasaki Y, Takami U, Shinohara U, Kurita K and Akiyoshi K 2007 *Biomacromolecules* **8** 2788
[107] Barrera D A, Zylstra E, Lansbury P and Langer R 1995 *Macromolecules* **28** 425
[108] Vunjak-Novakovic G, Obradovic B, Martin I, Bursac P M, Langer R and Freed L E 1998 *Biotechnol. Prog.* **14** 193
[109] Ishaug-Riley S L, Crane-Kruger G M, Yaszemski M J and Mikos A G 1998 *Biomaterials* **19** 1405
[110] Wald L, Sarakinos A G, Lyman M D, Mikos A G, Vacanti J P and Langer R 1993 *Biomaterials* **14** 270
[111] Iwasaki Y, Sawada S, Ishihara K, Khang G and Lee H B 2002 *Biomaterials* **23** 3897
[112] Liu C, Long L, Li Z, He B, Wang L, Wang J, Yuan X and Sheng J 2012 *J. Microencapsul.* **29** 242
[113] Saito A, Konno T, Ikake H, Kurita K and Ishihara K 2010 *Biomed. Mater.* **5** 054101
[114] Konno T and Ishihara K 2007 *Biomaterials* **28** 1770
[115] Xu Y, Jang K, Yamashita T, Tanaka Y, Mawatari K and Kitamori T 2012 *Anal. Bioanal. Chem.* **402** 99
[116] Xu Y, Sato K, Mawatari K, Konno T, Ishihara K and Kitamori T 2010 *Adv. Mater.* **22** 3017
[117] Kitano S, Koyama Y, Kataoka K, Okano T and Sakurai Y 1992 *J. Control. Release* **19** 161
[118] James T D, Sandanayake K R A S and Shinkai S 1994 *Angew. Chem., Int. Ed.* **33** 2207
[119] Miyata T, Uragami T and Nakamae K 2002 *Adv. Drug Deliv. Rev.* **54** 79
[120] Aikawa T, Konno T, Takai M and Ishihara K 2012 *Langmuir* **28** 2145
[121] Ishihara K 2000 *Sci. Technol. Adv. Mater.* **1** 131
[122] Iwasaki Y, Ishihara K and Nakabayashi N 1997 *Recent Res. Dev. Polym. Sci.* **1** 37
[123] Ishihara K 1997 TRIP **5** 401
[124] Hasegawa T, Iwasaki Y and Ishihara K 2002 *J. Biomed. Mater. Res.* **63** 333
[125] Iwasaki Y, Nakabayashi N and Ishihara K 2003 *J. Artif. Organs* **6** 260
[126] Ye S H, Watanabe J, Takai M, Iwasaki Y and Ishihara K 2005 *Biomaterials* **26** 5032
[127] Dahe G J, Kadam S S, Sabale S S, Kadam D P, Sarkate L B and Bellare J R 2011 *PLoS One* **6** e25236
[128] Ueda H, Watanabe J, Konno T, Takai M, Saito A and Ishihara K 2006 *J. Biomed. Mater. Res.* A **77** 19
[129] Myers G J, Johnstone D R, Swyer W J, McTeer S, Maxwell S L and Squires C 2003 *J. Extra Corpor. Technol.* **35** 6
[130] Yoneyama T, Ishihara K, Nakabayashi N, Ito M and Mishima Y 1998 *J. Biomed. Mater. Res.* **43** 15
[131] Yoneyama T, Ito M, Sugihara K, Ishihara K and Nakabayashi N 2000 *Artif. Organs* **24** 23
[132] Yoneyama T, Sugihara K, Ishihara K, Iwasaki Y and Nakabayashi N 2002 *Biomaterials* **23** 1455
[133] Soletti L, Nieponice A, Hong Y, Ye S H, Stankus J J, Wagner W R and Vorp D A 2011 *J. Biomed. Mater. Res.* A **96** 436

[134] Lewis A L, Furze J D, Small S, Robertson J D, Higgins B J, Taylor S and Ricci D R 2002 *J. Biomed. Mater. Res.* **63** 699
[135] Lewis A L, Willis S L, Small S A, Hunt S R, O'Byrne V and Stratford P W 2004 *Biomed. Mater. Eng.* **14** 355
[136] Iwasaki Y, Uchiyama S, Kurita K, Morimoto N and Nakabayashi N 2002 *Biomaterials* **23** 3421
[137] De S F, Van B Y, Caes F, François K, Arnout J, Bossuyt X, Taeyans Y and Van N G 2002 *Perfusion* **17** 39
[138] Schulze C J, Han L, Ghorpade N, Etches W S, Stang L, Koshal A and Wang S H 2009 *J. Card. Surg.* **24** 363
[139] Yamazaki K, Kihara S, Akimoto T, Tagusari O, Kawai A, Umezu M, Tomioka J, Kormos R L, Griffith B P and Kurosawa H 2002 *Japan J. Thorac. Cardiovasc. Surg.* **50** 461
[140] Kitao T *et al* 2011 *Artif. Organs* **35** 543
[141] Habara S *et al* 2011 *Int. Heart J.* **52** 88
[142] Grenadier E, Roguin A, Hertz I, Peled B, Boulos M, Nikolsky E, Amikam S, Kerner A, Cohen S and Beyar R 2002 *Catheter Cardiovasc. Interv.* **55** 303
[143] Deng M C, Edwards L B, Hertz M I, Rowe A W, Keck B M, Kormos R L, Naftel D C, Kirklin J K and Taylor D O 2005 *J. Heart Lung Transplant.* **24** 1182
[144] Ye S H, Johnson C A Jr, Woolley J R, Snyder T A, Gamble L J and Wagner W R 2009 *J. Biomed. Mater. Res.* A **91** 18
[145] Kihara S *et al* 2003 *Artif. Organs* **27** 188
[146] Snyder T A, Tsukui H, Kihara S, Akimoto T, Litwak K N, Kameneva M V, Yamazaki K and Wagner W R 2007 *J. Biomed. Mater. Res.* A **81** 85
[147] Yamazaki K, Saito S, Kihara S, Tagusari O and Kurosawa H 2007 *Gen. Thorac. Cardiovasc. Surg* . **55** 158
[148] Foy J R, Williams P F III, Powell G L, Ishihara K, Nakabayashi N and LaBerge M 1999 *Proc. Inst. Mech. Eng.* H **213** 5
[149] Moro T, Takatori Y, Ishihara K, Konno T, Takigawa Y, Matsushita T, Chung U I, Nakamura K and Kawaguchi H 2004 *Nat. Mater.* **3** 829
[150] Kyomoto M, Moro T, Konno T, Takadama H, Yamawaki N, Kawaguchi H, Takatori Y, Nakamura K and Ishihara K 2007 *J. Biomed. Mater. Res.* A **82** 10
[151] Kyomoto M, Moro T, Saiga K, Hashimoto M, Ito H, Kawaguchi H, Takatori Y and Ishihara K 2012 *Biomaterials* **33** 4451
[152] Kyomoto M, Moro T, Takatori Y, Kawaguchi H, Nakamura K and Ishihara K 2010 *Biomaterials* **31** 1017
[153] Goda T and Ishihara K 2006 *Expert Rev. Med. Devices* **3** 167
[154] Lewis A L and Lloyd A W 2012 *Biomimetic, Bioresponsive, Bioactive Materials: An Introduction to Integrating Materials with Tissues* ed M Santin and G J Phillips (Hoboken, NJ: Wiley) p 95

Trans. Mat. Res. Soc. Japan 37[3] 333-336 (2012)

Effects of dynamics of water molecules at hydrophilic polymer brush surfaces on protein adsorption behavior

Kazuomi Inoue[1], Yuuki Inoue*[1,3], and Kazuhiko Ishihara[1,2,3]

[1] Department of Materials Engineering, [2] Department of Bioengineering, School of Engineering, The University of Tokyo, Tokyo 113-8656, Japan,

[3] JST-CREST, Tokyo 102-0075, Japan

E-mail: inoue@mpc.t.u-tokyo.ac.jp

The suppression of protein adsorption must be required for a surface of biomaterials to avoid undesirable biological reactions. Understanding the interactions between proteins and surfaces is necessary to construct new biomaterials that have ultimate nonbiofouling property. Protein adsorption causes in an aqueous medium, therefore, we focused on the hydration state at the interface of the aqueous medium with proteins and the contacting materials, and investigated the effects of hydration state on protein adsorption behavior towards the surface. We could successfully establish the method for evaluation of dynamics of water molecules in the vicinity of the surface by using proton nuclear magnetic resonance spectroscopy for the hydrated polymer brush layer-modified micro-silica beads. The zwitterionic and cationic polymer brush surfaces were used for the measurement. The results clearly indicated that the dynamics of water molecules determined protein adsorption onto the surfaces. Thus, the polymer brush surfaces with hydration layer and high-diffusion of water molecules in the layer, such as phosphorylcholine group-bearing polymer brush surface, were effective to inhibit protein adsorption.

Key words: dynamics of water, protein adsorption, polymer brush structure, nuclear magnetic resonance, relaxation time

1. INTRODUCTION

Biological reactions, which are induced at a surface of materials when they contact with blood and tissues, such as thrombus formation, immunoresponse, and inflammatoric response, are initiated by protein adsorption on the surface [1]. Therefore, biomaterials surface requires quite strong inhibition for protein adsorption. The proteins interact with the materials surface by combination of various molecular forces generated in an aqueous medium. There is a hypothesis that shows protein adsorption would be caused by hydration layer with low motility [2]. In this regard, dynamics of water should be considered in order to realize zero protein adsorption surface. Some reports have attempted to clarify hydration state, and it was revealed that hydration state at the surface has strong effect on protein adsorption [3-8]. Among them, Ishihara *et al.* clearly demonstrated that the hydrophilic polymer surfaces with high-free water fraction reduced protein adsorption. That is, when the free-water fraction became up to 0.7, amount of protein adsorbed on the surface reduces below monolayer adsorption [3]. However, the role of water molecules at the protein-material interface is only guessed from static information of bulk water. Also, these previous reports were conducted using polymer coated surfaces, which have other difficulties for evaluation of water dynamics due to entanglement of polymer chains and entrapment of water molecules physically in the hydrated layer. From these points of view, we applied well-defined polymer brush surface with the controlled density and thickness of the polymer layer. The goal of this study is to understand the dynamics of water molecules focusing on the surface.

In this study, water that is coexisted with polymer chains in extended nanometer-space was acquired by using micro-silica beads covered with polymer brush layers [9, 10]. High-density polymer brush layers with various chemical structures were prepared on the micro-silica beads via surface-initiated atom transfer radical polymerization (SI-ATRP) [11]. Hydration state at the surfaces was evaluated by measurement of

relaxation time and diffusion coefficient using proton nuclear magnetic resonance spectroscopy (^{1}H-NMR) [12, 13]. Protein adsorption onto the surfaces was measured with a quartz crystal microbalance with dissipation monitoring (QCM-D) measurement [14, 15]. Finally, the relationship between protein adsorption and dynamics of water was discussed.

2. EXPERIMENTS

2.1. Materials

Three kinds of zwitterionic monomers and cationic one were used for making polymer brush surface. 2-Methacryloyloxyethyl phosphorylcholine (MPC) was synthesized and purified using a previously reported method [16]. [2-(Methacryloyloxy) ethyl] dimethyl (3-sulfopropyl) ammonium hydroxide (SBMA) was purchased from Sigma-Aldrich Co. (St. Louis, USA). *N*-Methacryloyloxyethyl *N*, *N*-dimethyl ammonium -α-*N*-methyl carboxylate (CBMA) was obtained from Wako Pure Chemistry (Osaka, Japan). Trimethyl-2-methacroyloxyethylammonium Chloride (TMAEMA) was purchased from Tokyo Chemical Industry Co., Ltd. (Tokyo, Japan). Copper (I) bromide (CuBr), 2,2′-bipyridyl (bpy), and ethyl-2-bromoisobutyrate (EBIB) were purchased from Sigma–Aldrich Co. and were directly used as received. All other reagents and solvents of extra-pure grade were commercially available and were directly used as purchased. Micro-silica beads with 10-μm in diameter were purchased from Fuji Silysia Chemical Ltd. (Aichi, Japan).

2.2. Preparation of initiator immobilized beads

The surface-immobilizing initiator for SI-ATRP, (11-(2-bromo-2-methyl) propionyloxy) undecyltrichlorosilane (BrC10TCS) was synthesized using a previously described method [11, 17]. The micro-silica beads were etched using piranha solution, which is consisted of 30 % of hydrogen peroxide and 70 % of sulfuric acid, for 15 min. The silica beads were removed from the solution and washed with plenty of distilled water. The cleaned silica beads were immersed in a 5 mmol/L solution of BrC10TCS in toluene for 24 h. The BrC10TCS-immobilized silica beads were removed from the solution, rinsed with toluene and methanol, and dried in a dry box under reduced pressure.

2.3. Preparation of polymer brush-modified beads

MPC, SBMA, CBMA, and TMAEMA were graft polymerized from the BrC10TCS-immobilized silica beads using SI-ATRP as follows: CuBr, bpy, and each monomer in a particular molar ratio were placed in a glass tube and dehydrated; thereafter, degassed solvents were added into the glass tube. The following solvents were used: ethanol for MPC and CBMA at a monomer concentration of 0.56 mol/L, a mixture of methanol and water (50:50 by volume %) for SBMA at a monomer concentration of 0.38 mol/L, and a mixture of methanol and water (70:30 by volume %) for TMAEMA at a monomer concentration of 1.0 mol/L. Sodium chloride of the same concentration as SBMA (0.38 mol/L) was added to the SBMA solution to prevent the precipitation of poly(SBMA) during polymerization. Argon was bubbled into each monomer solution at room temperature for 10 min. The BrC10TCS-immobilized silica beads were then immersed into the solution, and EBIB was simultaneously added as the free initiator at one-fiftieth of monomer concentration. After the glass tubes were sealed, polymerization was performed at 20 °C with stirring. After 24 h, the obtained silica beads were removed from the polymerization solution using centrifugation, rinsed with solvents (ethanol for poly(MPC) and poly(CBMA), sodium chloride solution for poly(SBMA), and water for poly(TMAEMA)), and dried in a dry box under reduced pressure. The structure of the polymer brush surface was shown in Fig. 1.

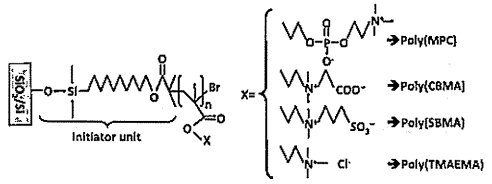

Fig. 1. Chemical structures of polymer brush surface.

2.4. Analysis of hydration state

2.4.1. Measurement of diffusion coefficient

The polymer brush layer-modified silica beads (500 mg) were packed into NMR tubing (ϕ = 10 mm, JEOL, Tokyo, Japan) and distilled water (500 μL) was added into the NMR tubing. Diffusion coefficient (D) measurement of water molecules was performed using ^{1}H-NMR (MU-25, JEOL, Tokyo, Japan) with pulse field gradient method. The D value is an indication of motility of water molecules. The interspaces among the silica beads are extremely small, therefore, we can investigate only water molecules in the vicinity of the polymer brush surface [9, 10].

2.4.2. Evaluation of hydration layer

In order to evaluate the diffusing range of hydrated layers around polymer brush surfaces, relaxation time of water molecules was measured about three types of

samples as followed (Fig. 2). The polymer brush layer-modified silica beads were packed into an NMR tube and distilled and degassed water was added into the tube (type-1). The polymer brush layer-modified silica beads were damped with vapor of saturated sodium chloride solution (RH=75%) and packed into an NMR tube (type-2). Distilled water was degassed with vacuum, and poured into an NMR tube (type-3). Spin-lattice relaxation time (T_1 value) of water molecules was measured using ^{1}H-NMR with inversion recovery method. We defined T_1 for type-1 as T_{1liq}, T_1 for type-2 as T_{1vap}, and T_1 for type-3 as T_{1bulk}, respectively. We presumed that hydration state in liquid water around the polymer brush layer (type-1) would be regarded as a overlap of hydration state of the polymer brush layer only (type-2) and that of a bulk water (type-3). In the case that contains the multi-components of T_1 value, the following equation is generally used [9].

$$1 / T_{1liq} = \alpha / T_{1vap} + (1-\alpha) / T_{1bulk}$$

We hypothesized that the α value would represent the diffusing range of hydrated layers around polymer brush surfaces in liquid water. In this study, the α values were calculated at the several kinds of the polymer brush surface.

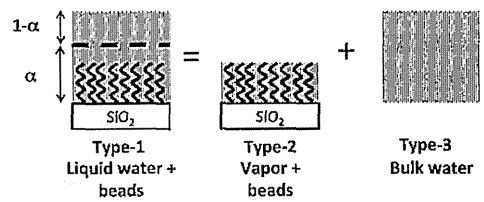

Fig. 2. Samples for evaluation of diffusing range of hydrated layer.

2.5. Protein adsorption measurement

The adsorbed amount of proteins from 100% fetal bovine serum (FBS) on the polymer brush surfaces at 37 °C was quantified using QCM-D measurement (Q-Sense, Gothenburg, Sweden) [14, 15, 17]. To measure the protein adsorption mass on the surface, the polymer brush layers were formed at the surface of QCM-D gold sensor. The following equation was used to estimate the adsorbed amount of protein on the polymer brush surface.

Protein adsorption amount (ng/cm^2) =
17.7 x Frequency shift value (Hz)

3. RESULTS AND DISCUSSION

3.1. Hydration state

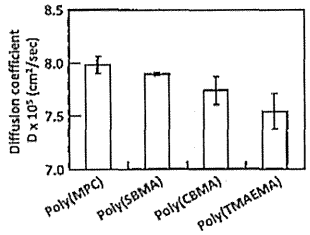

Fig. 3. Diffusion coefficient of water molecules in various hydrated polymer brush system.

Fig. 3 shows the diffusion coefficient (D) values of water at various polymer brush layer-modified silica beads system. The zwitterionic polymer brush surfaces had higher diffusion coefficient compared to the cationic one. In particular, poly(MPC) brush surface had a larger D value. This result means that water molecules near poly(MPC) brush surface has a high motility. On the other hand, the motility of water molecules near poly(TMAEMA) brush surface was restrained. Recently, Takahara *et al.* reports the solubilizing state and dimension of polymer chains in several polymer brush layers in an aqueous medium. In this report, the poly(MPC) chains expanded in the aqueous medium well and the dimension of poly(MPC) chains was not changed by the ionic strength of the aqueous medium [18]. It is well known that the polymer chains shrink in an aqueous medium with ions because the ions would extract water molecules hydrated at polymer chains. The relatively high D value of water molecules and well-expanded structure of the poly(MPC) chains in ionic medium indicated that water molecules may be bounded quite weakly with the poly(MPC) chains.

Fig. 4 shows the diffusing range of hydrated layer (α values) at several polymer brush surfaces. Cationic poly(TMAEMA) surface had larger hydration layer than zwitterionic polymer surfaces. This result can be explained by two effects. First, the poly(TMAEMA) chains expands in an aqueous medium much wider than zwitterionic polymer chains due to strong electrostatic repulsion forces among cationic charges. Second, water molecules strongly hydrated surrounding each poly(TMAEMA) chain [19]. It is difficult to distinguish these effects in the present time, we are now evaluating

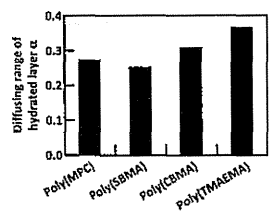

Fig. 4. Diffusing range of hydrated layer at several polymer brush surfaces.

the real number of water molecules bounded on the monomer unit in the polymer chains.

3.2. Relationship between protein adsorption and dynamics of water

As seen in Fig. 5, we determined the relationship between protein adsorption and dynamics of water at the polymer brush surfaces. The polymer brush surface with larger diffusion coefficient resisted protein adsorption. Particularly, large amount of protein adsorbed on poly(TMAEMA) brush surface. Compared to the theoretical monolayer adsorption mass, the multilayer adsorption would occur on the cationic polymer brush surface. The multilayer adsorption would be promoted at the cationic surface because of both electrostatic interaction and its thick hydration layer with lower motility of water molecules around the cationic surface. These effects would be due to the outstanding difference in protein adsorption mass between on the cationic surface and zwitterionic surfaces.

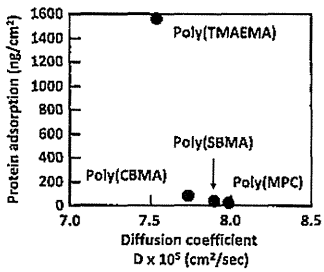

Fig. 5. Relationship between the adsorbed amount of proteins and diffusion coefficient of water molecules .

4. CONCLUSION

We researched the effect of molecular dynamics of water on protein adsorption behavior on well-defined polymer brush surface. First, we could successfully fabricate the polymer brush layers with varying chemical structures. Then, the surface-specific hydration state could be evaluated using the relaxation time measurement of water enclosed among the micro-silica beads. It is clarified that the zwitterionic polymer brush layers would be effective to reduce interaction with proteins. Interrelation between protein adsorption and hydration state at the materials surface was suggested. Control of polymer brush layer at the surface focusing on the dynamics of water molecules will realize the zero protein adsorption surfaces.

Acknowledgements

We thank to Prof. Madoka Takai, The University of Tokyo and Dr. Takehiko Tsukahara, Tokyo Institute of Technology, for their hearty and constructive discussions for this research.

References

[1] H. Chen, L. Yuan, W. Song, Z. Wu, D. Li, *Prog. Polym. Sci.* 33 (2008) 1059–1087.

[2] D. R. Lu, S. J. Lee, K. Park: *J. Biomater. Sci. Polym. Edn.* 3 (1991) 127-147

[3] K. Ishihara, H. Nomura, T. Mihara, K. Kurita, Y. Iwasaki, N. Nakabayashi, *J. Biomed. Mater. Res.* 39 (1998) 323-330.

[4] H. Kitano, K. Sudo, K. Ichikawa, M. Ide, K. Ishihara, *J. Phys. Chem.* 104 (2000) 10425-10429

[5] H. Kitano, M. Imai, T. Mori, M. Gemmei-Ide, Y. Yokoyama, K. Ishihara, *Langmuir* 19 (2003) 10260-10266.

[6] H. Kitano, S. Tada, T. Mori, K. Takaha, M. Gemmei-Ide, M. Tanaka, M. Fukuda, Y. Yokoyama, *Langmuir* 21 (2005) 11932-11940.

[7] M. Tanaka, A. Mochizuki, *J. Biomed. Mater. Res. A* 68 (2004) 684-695.

[8] S. Morita, M. Tanaka, Y. Ozaki, *Langmuir* 23 (2007) 3750-3761.

[9] T. Tsukahara, W. Misutani, K. Mawatari, T. Kitamori, *J. Phys. Chem. B* 113 (2009) 10808-10816.

[10] T. Tsukahara, A.Hibara, Y. Ikeda, T. Kitamori, *Angew. Chem.* 46 (2007) 1180-1183.

[11] K. Matyjaszewski, P. Miller, N. Shukla, B. Immaraporn, A. Gelman, B. Luokala, T. Siclovan, G. Kickelbick, T. Vallant, H. Hoffmann, T. Pakula, *Macromolecules* 32 (1999) 8716-8724.

[12] T. Ohkubo, H. Kikuchi, M. Ymaguchi, *Phys. Chem. Earth* 33 (2008) 169-176.

[13] X. Guichet, M. Fleury, E. Kohler, *J. Colloid Interface Sci.* 327 (2008) 84-93.

[14] A. Dolatshahi-Pirouz, K. Rechendorff, M. B. Hovgaard, M. Foss, J. Chevallier, F. Besenbacher, *Colloids Surf. B: Biointerfaces* 66 (2008) 53–59.

[15] A.G. Hemmersam, M. Foss, J. Chevallier, F. Besenbacher, *Colloids Surf. B: Biointerfaces* 43 (2005) 208–215.

[16] K. Ishihara, T. Ueda, N. Nakabayashi, *Polym. J.* 22 (1990) 355–360.

[17] Y. Inoue, K. Ishihara, *Colloids Surf. B: Biointerfaces* 81 (2010) 350–357.

[18] M.Kikuchi, Y.Terayama, T. Ishikawa, T. Hoshino, M. Kobayashi, H. Ogawa, H.Masunaga, J-I. Koike, M. Horigome, K. Ishihara, A. Takahara, *Polym. J.*, 44 (2012) 121-130.

[19] M. Kobayashi, H. Yamaguchi, Y. Terayama, Z. Wang, K. Ishihara, M. Hino, A. Takahara, *Macromol. Sympo.* 279 (2009) 79-87.

(Received 15 January 2012; Accepted 27 May 2012)

(Received 15 January 2012; Accepted 27 May 2012)

Society For Biomaterials

Calcium-incorporated titanium surfaces influence the osteogenic differentiation of human mesenchymal stem cells

Rumi Sawada,[1] Ken Kono,[1] Kazuo Isama,[2] Yuji Haishima,[1] Atsuko Matsuoka[1]

[1]Division of Medical Devices, National Institute of Health Sciences, Tokyo, Japan
[2]Division of Environmental Chemistry, National Institute of Health Sciences, Tokyo, Japan

Received 21 September 2012; accepted 13 December 2012
Published online 11 February 2013 in Wiley Online Library (wileyonlinelibrary.com). DOI: 10.1002/jbm.a.34566

Abstract: In this study, a titanium surface was chemically modified with calcium ions and assessed for its influence on osteogenic differentiation and molecular responses of human mesenchymal stem cells (hMSCs). Titanium disks were treated with NaOH (NaOH treatment), NaOH + $CaCl_2$ ($CaCl_2$ treatment), or NaOH + $Ca(OH)_2$ ($Ca(OH)_2$ treatment). $Ca(OH)_2$ treatment caused significantly greater calcium incorporation onto the titanium surface and apatite formation than $CaCl_2$ treatment. The morphology of hMSCs differed on $CaCl_2$- and $Ca(OH)_2$-treated disks. The osteopontin (OPN) expression in hMSCs cultured on $CaCl_2$-treated titanium was significantly higher than that in cells cultured on NaOH-treated disks; OPN expression was significantly higher in cells cultured on $Ca(OH)_2$-treated disks than on un-, NaOH-, and $CaCl_2$-treated disks. Osteocalcin (OCN) protein expression in hMSCs cultured on $Ca(OH)_2$-treated disks was significantly higher than that on all the other disks. Comparative expression profiling by DNA microarray and pathway analyses revealed that calcium modification of the titanium surface induced integrin β3 after OPN upregulation and promoted Wnt/β-catenin signaling in hMSCs. In addition, $Ca(OH)_2$ treatment upregulated the expression of bone morphogenetic protein 2, cyclooxygenase 2, and parathyroid hormone-like hormone in comparison to $CaCl_2$ treatment. These observations suggest that calcium-modified titanium surfaces affect osteogenic differentiation in hMSCs and that $Ca(OH)_2$ treatment induced osteogenic differentiation in hMSCs, whereas $CaCl_2$ treatment had a limited effect. © 2013 Wiley Periodicals, Inc. J Biomed Mater Res Part A: 101A: 2573–2585, 2013.

Key Words: surface modification, titanium, calcium, stem cell, osteogenesis, gene expression

How to cite this article: Sawada R, Kono K, Isama K, Haishima Y, Matsuoka A. 2013. Calcium-incorporated titanium surfaces influence the osteogenic differentiation of human mesenchymal stem cells. J Biomed Mater Res Part A 2013:101A:2573–2585.

INTRODUCTION

Titanium is widely used in orthopedic and dental implants due to its corrosion and wear resistance, durability, and biocompatible interface. The topography of titanium implants plays a major role in cell–material interaction. Several studies have shown that surface modifications influence protein adsorption,[1,2] cell–substrate interactions,[3] cell adhesion,[3–5] cell morphology,[5,6] osteogenic differentiation,[5,7–10] and, consequently, the tissue integration of titanium implants.[11,12]

The nanoscale and microscale surface roughness of titanium has been reported to increase osteogenic differentiation in osteoblasts cultured on titanium surfaces[7,9–12] and promote osteogenic differentiation in human mesenchymal stem cells (hMSCs) in the presence of osteogenic supplements.[8] Osteoblast response has also been reported to be modulated by a modified microstructured titanium surface with increased wettability due to a polyelectrolyte thin film coating.[13] Titanium nanopores also affect osteogenic differentiation and hMSC cell morphology.[5] Integrin is critical for the responses of osteoblasts[4,10,14] and hMSCs[5] to some titanium surface modifications. Gene expression studies have shown an increase in the expression of the osteoinductive genes RUNX2, osterix, alkaline phosphatase, bone sialoprotein, and osteocalcin (OCN) in osteoblasts[6,15] and hMSCs[16,17] grown on micro- and nanoroughened surfaces in the presence of osteogenic supplements.

Alkali- and heat-treated titanium forms a bone-like apatite surface layer in the body and bonds to the bone via this layer.[18–22] In addition to chemical and thermal treatments, the porous structure of titanium contributes to its biocompatibility[23] and bone formation[24] *in vivo*. Fluoride ion modification of a TiO_2 grit-blasted surface enhances osteoblastic differentiation in hMSCs in the presence of osteogenic supplements.[25] Calcium ion incorporation into a titanium surface by $CaCl_2$ treatment yields slightly better apatite formation than alkali (NaOH) treatment *in vitro*,[26] but the influence of calcium ion modifications of titanium surfaces on osteogenic differentiation of hMSCs has not been explored.

hMSCs are pluripotent and can differentiate into cells of mesodermal origin, for example, bone, cartilage, adipose,

Correspondence to: R. Sawada; e-mail: rsawada@nihs.go.jp
Contract grant sponsor: Health and Labour Sciences Research Grants for Research on Regulatory Science of Pharmaceuticals and Medical Devices from the Ministry of Health, Labour and Welfare of Japan; contract grant numbers: H22-IYAKU-IPPAN-009, H24-IYAKU-SHITEI-018

and muscle cells.[27–31] hMSCs also have the capacity to differentiate into myocytes,[32,33] hepatocytes,[27,34] and neural cells.[29] hMSCs are currently being used with biomedical materials in several clinical studies on bone regeneration.

We aimed to evaluate the influence of $CaCl_2$- or $Ca(OH)_2$-modified titanium surfaces on osteogenic differentiation and molecular responses in hMSCs. We examined the amount of calcium ion incorporation and apatite formation on $CaCl_2$- and $Ca(OH)_2$-treated surfaces. We investigated the morphology, proliferation, and osteogenic differentiation of hMSCs cultured on the chemically modified titanium. To definitively conclude whether incorporation of calcium ions on a titanium surface induces osteogenic differentiation in hMSCs, osteogenic supplements were not used in this study. Whole genome expression analysis provided a comprehensive understanding of the mechanism of osteogenic induction by chemically modified titanium.

MATERIALS AND METHODS

Chemical treatment of titanium disks

Titanium disks (grade II commercially pure titanium, 33.5 mm diameter, 2-mm thick) were supplied by Nakashima Medical Co. (Okayama, Japan). They contain over 99.3075% of titanium, and their surface roughness (Ra) is 0.4 μm. NaOH treatment was performed by soaking the disks in 5.0 mol/L NaOH aqueous solution at 60°C for 24 h and then washing gently with distilled water. $CaCl_2$ or $Ca(OH)_2$ treatments were performed by soaking the NaOH-treated disks in 0.1 mol/L $CaCl_2$ or 0.01 mol/L $Ca(OH)_2$ at 60°C for 24 h and then gently washing with distilled water. Untreated titanium disks served as controls.

Scanning electron microscopy

The topography of the chemically modified titanium disks was characterized by Scanning electron microscopy (SEM) performed with a JSM-5800 microscope (JEOL, Tokyo, Japan). Images were recorded with 15 kV accelerating voltage.

Calcium ion incorporation and apatite formation

To investigate apatite formation on the titanium surface, untreated or chemically modified disks were soaked in Hanks' balanced salt solution that included calcium and magnesium (Life Technologies Co., Carlsbad, CA) for 7 days at 37°C. The solution was changed every 2 days.

The incorporated calcium ions were dissolved in nitric acid and their concentration was measured by Agilent 7500ce ORS ICP-MS (inductively coupled plasma mass spectrometry; Agilent, Santa Clara, CA) in helium collision mode with monitoring at m/z 43.

Cell culture

hMSCs derived from bone marrow were purchased from Lonza (Walkersville, MD). The hMSCs were cultured in MSCGM BulletKit, a mesenchymal stem cell basal medium with mesenchymal cell growth supplement, L-glutamine, and gentamycin/amphotericin-B (Lonza Walkersville, MD), at 37°C under a 5% CO_2 atmosphere. The medium was changed every 3 days. The cells were detached by mild treatment with trypsin/ethylenediaminetetraacetic acid solution for hMSCs (Lonza Walkersville, MD) and subcultured when they were just subconfluent (approximately 80–90% confluence). Cell passages 2–4 were used for experiments. hMSCs were cultured on each surface-modified titanium disk for 1, 4, 7, and 28 days.

Cell morphology and immunofluorescence staining

To analyze the morphology of hMSCs cultured on the chemically modified titanium disks, the cells were stained with CellTracker (Lonza) according to the manufacturer's protocol.

To examine the expression of OCN, cells stained with CellTracker were fixed with 4% paraformaldehyde in phosphate buffered saline (PBS) for 15 min at room temperature and permeabilized with a blocking solution [10% normal donkey serum (Jackson ImmunoResearch Laboratories, Baltimore, PA), 0.1% Triton X-100, and 0.01% NaN_3 in PBS]. The cells were stained with anti-OCN antibody (Abcam, Cambridge, MA) in blocking solution without Triton X-100 for 16 h at 4°C for primary staining and were secondarily stained with Alexa Fluor 647-conjugated donkey anti-mouse antibody (Jackson ImmunoResearch Laboratories) for 30 min at room temperature.

Images were collected and analyzed by confocal microscopy (FLUOVIEW FV1000; Olympus, Tokyo, Japan).

Cell proliferation

The proliferation of hMSCs on titanium disks for 7 days was determined by using a cell proliferation assay reagent, TetraColor ONE (Seikagaku Co., Tokyo, Japan). Cultures were incubated for 2 h in medium containing the reagent. The absorbance was read at 450 nm (reference at 600 nm) on a plate reader (SH-9000, Corona Electric Co., Ibaraki, Japan).

Preparation of total RNA and real-time polymerase chain reaction

hMSCs were seeded on untreated and chemically modified titanium disks in 35 mm culture dishes at an initial seeding density of 1.2×10^4 cells/cm^2 and cultured for 7 days before evaluating transcript expression of osteopontin (OPN), OCN, and glyceraldehyde-3-phosphate dehydrogenase (GAPDH). The housekeeping gene GAPDH was used as a control. Total RNA was extracted from hMSCs with the RNeasy Mini Kit (QIAGEN, Valencia, CA). Total RNA was eluted in RNase-free water and quantified on a NanoDrop 1000 spectrophotometer (Thermo Scientific, Wilmington, DE). Total RNA was reverse transcribed with the SuperScript III First-Strand Synthesis System for real-time polymerase chain reaction (RT-PCR; Life Technologies Co., Carlsbad, CA). Amplification of OPN, OCN, and GAPDH was performed with LightCycler Primer Sets (Roche Applied Science, Basel, Switzerland) and LightCycler Fast Start DNA Master SYBR Green I (Roche Applied Science) in a Roche LightCycler instrument (software version 4.0).

Microarray analysis

Whole genome expression was analyzed after 7-day culture of hMSCs on chemically modified titanium disks. Total RNA

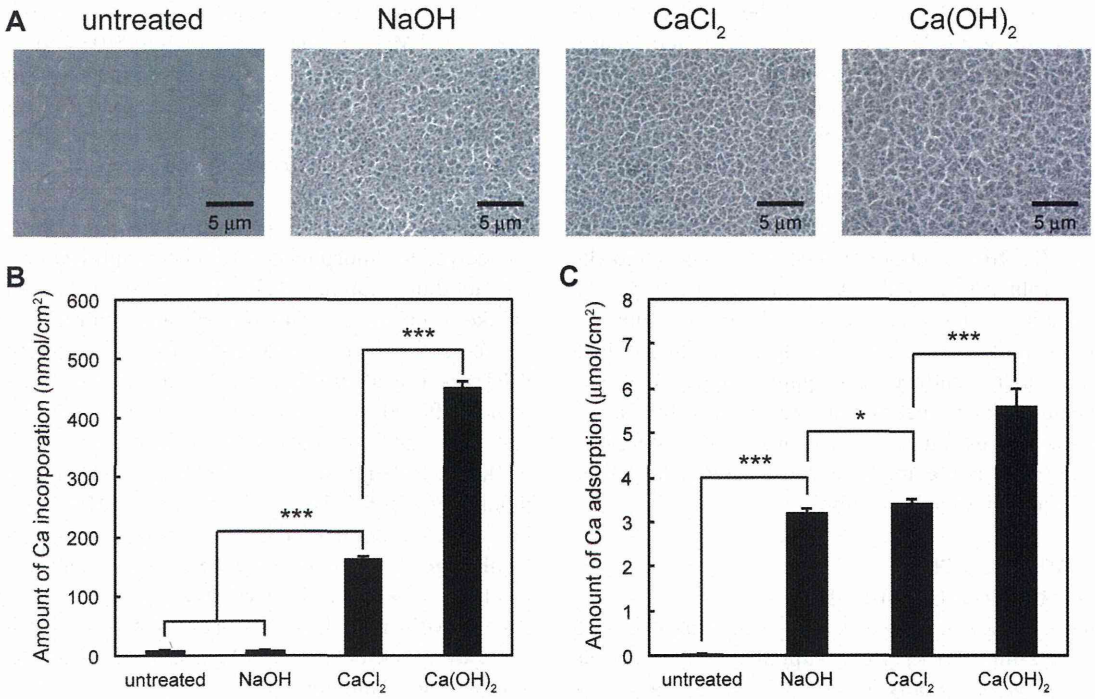

FIGURE 1. SEM images of the surface of untreated, NaOH-, NaOH + $CaCl_2$ ($CaCl_2$)-, and NaOH + $Ca(OH)_2$ ($Ca(OH)_2$)-treated titanium disks (A). Images are representative of three independent experiments. The amount of Ca^{2+} incorporation into the chemically modified titanium disks (B; left) and the amount of Ca^{2+} adsorption onto the modified disks after soaking in Hanks' balanced salt solution including calcium and magnesium at 37°C for 7 days (B; right) were measured by ICP-MS ($n = 3$). Significant differences between groups are shown as $^{*}p < 0.05$ and $^{***}p < 0.001$.

quantity and quality were assessed on an Agilent 2100 Bioanalyzer (Agilent, Santa Clara, CA); 100 ng of total RNA was used to generate biotin-modified amplified RNA (aRNA) with the GeneChip 3'IVT Express Kit (Affymetrix, Santa Clara, CA). Reverse transcription of first-strand complementary DNA (cDNA) with a T7 promoter sequence was performed with T7 oligo(dT) primer. Second-strand cDNA synthesis was used to convert the single-stranded cDNA into a double-stranded DNA template. The reaction employed DNA polymerase and RNase H to simultaneously degrade the RNA and synthesize second-strand cDNA. *In vitro* transcription of biotin-modified aRNA with IVT Labeling Master Mix generated multiple copies of biotin-modified aRNA from the double-stranded cDNA templates. The aRNA was purified and quantified; after fragmentation, it was hybridized to the GeneChip Human Genome U133 Plus 2.0 Array (Affymetrix). The arrays were stained with phycoerythrin and washed at the GeneChip Fluidics Station 450 (Affymetrix). The microarrays were scanned and data extracted using GeneChip scanner 3000 7G (Affymetrix), image analysis was performed using the Affymetrix GeneChip Command Console Software and digitized using Affymetrix Expression Console.

Data processing and pathway analysis

Data analysis was performed with GeneSpring GX 11.0 software (Agilent Technologies, Santa Clara, CA). Raw data were normalized to the 50th percentile per chip and the median per gene. Normalized means for the four kinds of titanium disks (un-, NaOH-, $CaCl_2$-, or $Ca(OH)_2$-treated) were generated for the experimental interpretation. Differentially expressed genes were selected and flagged for further analysis. To determine whether particular osteogenic differentiation functions were significantly overrepresented, the data set was analyzed using Ingenuity Pathway Analysis (IPA) 9.0 (Ingenuity Systems, Redwood City, CA).

Statistical analysis

All results are shown as means ± SD. Significance was evaluated by the Student's *t* test.

RESULTS

Surface characterization of chemically modified titanium disks

Titanium disks were treated with NaOH (NaOH treatment), NaOH + $CaCl_2$ ($CaCl_2$ treatment), and NaOH + $Ca(OH)_2$ ($Ca(OH)_2$ treatment; see Materials and methods section). SEM demonstrated a porous network structure formed on the surface of the disks after chemical treatment [Fig. 1(A)]. There were no significant differences between the chemically treated surfaces.

Calcium ion incorporation and apatite formation on the titanium surface

We measured the amount of calcium ion incorporation on the surface of the modified titanium disks [Fig. 1(B)]. As expected, no calcium ions were incorporated into the untreated or NaOH-treated disks. Significantly more calcium ions were incorporated into the $Ca(OH)_2$-treated disks than the $CaCl_2$-treated disks.

To investigate the effects of chemical treatments on apatite formation on the titanium surface, the disks were

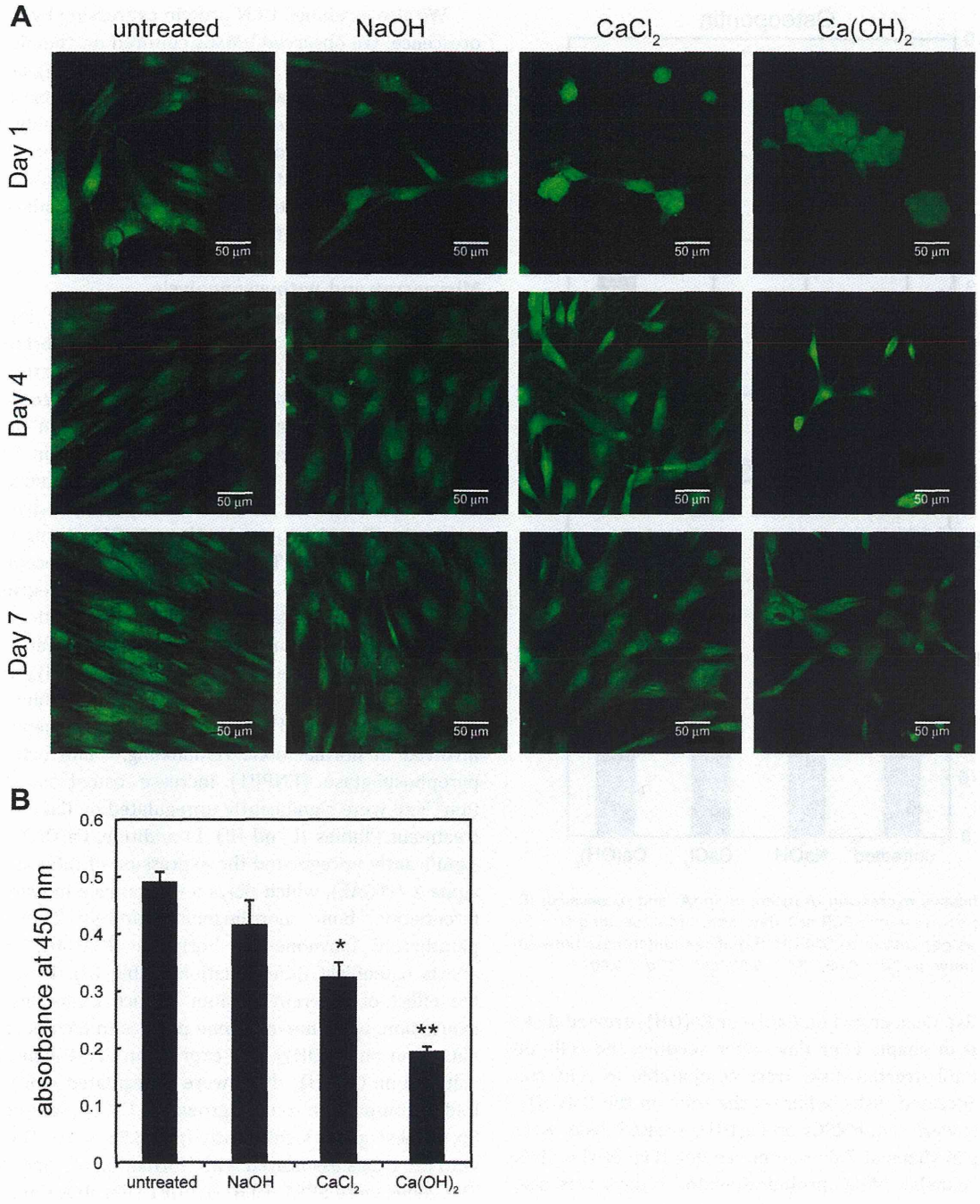

FIGURE 2. Confocal microscopy of hMSCs cultured on untreated, NaOH, $CaCl_2$, and $Ca(OH)_2$ treated titanium disks for 1, 4, and 7 days (A). Images are representative of five independent experiments. Cells were stained with CellTrackerTM Green Fluorescent Probe (Lonza). Proliferation of hMSCs for 7 days was determined with the cell proliferation assay reagent TetraColor One (B). The optical density of each well was measured at 450 nm ($n = 3$). Significant differences in comparison to untreated titanium are shown as $^*p < 0.05$ and $^{**}p < 0.01$. [Color figure can be viewed in the online issue, which is available at wileyonlinelibrary.com.]

soaked in Hanks' Balanced Salt Solution for 7 days. The amount of Ca^{2+} on titanium disks treated with NaOH, $CaCl_2$, and Ca(OH) was directly correlated with apatite formation. Apatite formation was slightly but significantly greater on $CaCl_2$-treated disks than on NaOH-treated disks [Fig. 1(C)]. Furthermore, $Ca(OH)_2$-treated titanium disk caused significantly greater apatite formation than the NaOH- and $CaCl_2$-treated disks [Fig. 1(C)].

Cell morphology and proliferation

To understand cell adhesion, we investigated the morphologies of hMSCs cultured on chemically modified titanium disks. We labeled the cells with CellTracker (Lonza) and observed at 1, 4, and 7 days after seeding. Confocal microscopy revealed cells on the modified disks showed smaller spread areas 1 day after seeding, although cells on the untreated disks exhibited normal cell morphology [Fig. 2(A)

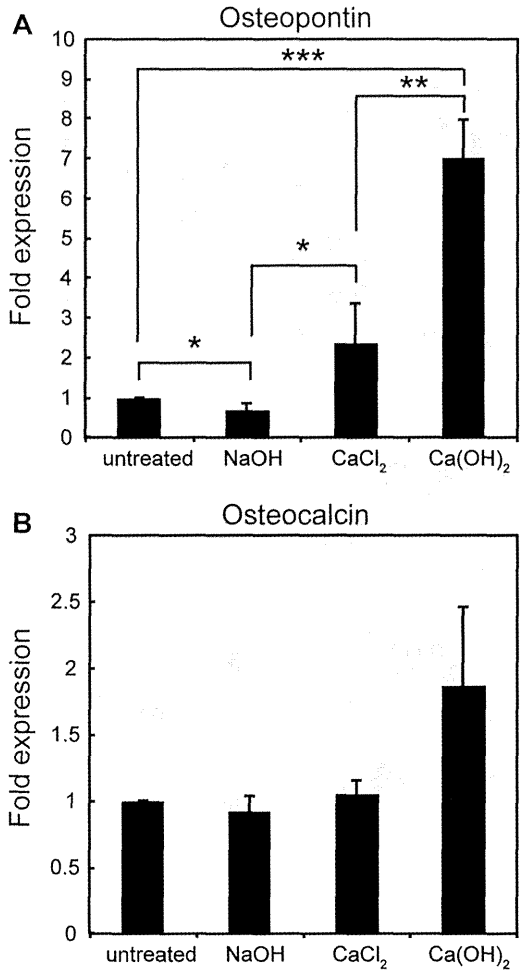

FIGURE 3. Relative expression of osteopontin (A) and osteocalcin (B) were analyzed by real-time PCR at 7 days after hMSC seeding ($n = 3$). The value was normalized to GAPDH. Significant differences between groups are shown as $^{*}p < 0.05$, $^{**}p < 0.01$, and $^{***}p < 0.001$.

upper panels]. Cells grown on $CaCl_2$- or $Ca(OH)_2$-treated disks were round in shape. Four days after seeding, the cells on NaOH- or $CaCl_2$-treated disks were comparable to cells cultured on untreated disks, whereas the cells on the $Ca(OH)_2$-treated disk were not. hMSCs on $Ca(OH)_2$-treated disks were comparable in shape at 7 days after seeding [Fig. 2(A) middle and lower panels]. hMSC proliferation for 7 days was also investigated. Culture on chemically modified titanium surfaces decreased hMSC cell numbers [Fig. 2(B)].

Cell differentiation and quantitative real-time PCR

To investigate the osteogenic differentiation of hMSCs cultured on chemically modified titanium disks, OPN and OCN transcripts were characterized by real-time PCR after culture for 7 days (Fig. 3). The transcript levels of OPN in hMSCs cultured on $CaCl_2$-treated titanium disks were significantly higher than those on NaOH-treated disks [Fig. 3(A)]. OPN expression was significantly greater on $Ca(OH)_2$-treated disks than on un-, NaOH-, and $CaCl_2$-treated disks [Fig. 3(A)]. OCN expression on $Ca(OH)_2$-treated disks was slightly higher than on the other treated disks [Fig. 3(B)].

We also examined OCN protein expression by immunofluorescence. We observed hMSCs cultured on chemically modified titanium for 7, 14, 21 days (data not shown), and 28 days [Fig. 4(A)]. Although we did not detect expression on all cells until 21 days after seeding (data not shown), only hMSCs on the $Ca(OH)_2$-treated disks showed OCN expression 28 days after seeding [Fig. 4(B)]. The fluorescence intensity of hMSCs cultured on $Ca(OH)_2$-treated titanium was significantly stronger than on the other treated disks [Fig. 4(C)].

Microarray and pathway analysis

To investigate the mechanism of osteogenic induction in hMSCs by chemically modified titanium, we performed DNA microarray analysis. We analyzed mRNA extracted from hMSCs cultured on chemically modified titanium for 7 days. The top 30 genes significantly upregulated on treated versus untreated titanium disks are summarized in Tables I–III. A significant change was defined as a difference of more than twofold relative to the control. Differentially expressed genes significantly upregulated on NaOH versus nontreated disks are shown in Table I. Interleukin 6 receptor (IL6R) increases osteoblast differentiation, and integrin, beta 1 (ITGB1) plays a critical role in the process; both were significantly upregulated on NaOH-treated disks (Table I). Genes significantly upregulated by $CaCl_2$ or $Ca(OH)_2$ treatments versus the untreated control are shown in Tables II and III. SPP1 (OPN) and MMP13 (matrix metallopeptidase 13), involved in normal bone remodeling,[35] and ectonucleotide pyrophosphatase (ENPP1) increase osteoblast differentiation[36]; all were significantly upregulated by $CaCl_2$ or $Ca(OH)_2$ treatment (Tables II and III). In addition, $Ca(OH)_2$ treatment significantly upregulated the expression of IL6R and integrin, alpha 2 (ITGA2), which plays a critical role in osteoblast differentiation, bone morphogenetic protein 2 (BMP2), and parathyroid hormone-like hormone (PTHLH), which also affects osteoblast differentiation (Table III). To differentiate the effect of different calcium surface treatments on gene expression, we compared gene profiles in hMSCs cultured on $CaCl_2$ and on $Ca(OH)_2$. The expression of 94 genes in hMSCs cultured on $Ca(OH)_2$ disks were upregulated more than twofold in comparison to cells grown on $CaCl_2$ (data not shown). Six of these genes significantly ($p = 3.96 \times 10^{-4}$) overlapped with the genes associated with "formation of bone" in the IPA. The genes were SPP1, PTHLH, FGF1 (fibroblast growth factor 1), BMP2, PTGS1 (cyclooxygenase 1), and PTGS2 (cyclooxygenase 2; Cox2) (Table IV).

To determine the significance of the effects of different titanium treatments on osteogenic differentiation in hMSCs, we used IPA. Differentially expressed genes that were significantly influenced by NaOH, $CaCl_2$, or $Ca(OH)_2$ treatment were compared with untreated controls in the canonical pathway defined by IPA in osteoblast and are shown in Figures 5–7. Genes that were not detected in untreated controls, but were detected in hMSCs cultured on chemically modified titanium are represented as "induced genes" in these figures. Genes that were detected in untreated controls but not in hMSCs grown on chemically modified titanium are indicated as "suppressed genes". The NaOH-treated titanium surface induced

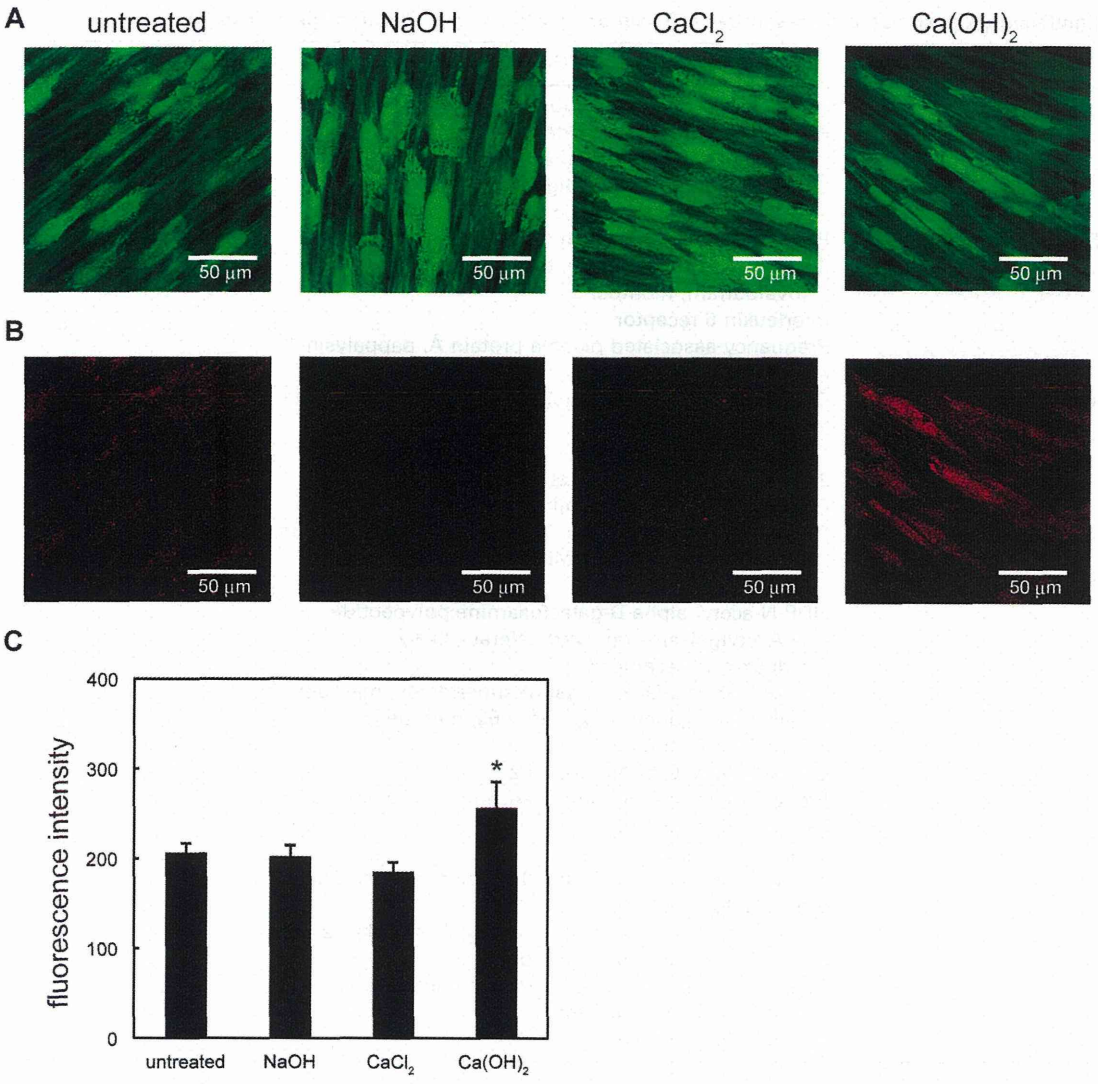

FIGURE 4. Confocal microscopy of hMSCs (A) and osteocalcin in hMSCs (B) cultured on chemically modified titanium disks for 28 days. Green: CellTrackerTM Green Fluorescent Probe; red: Alexa Fluor 647 donkey anti-mouse. Images representative of three independent experiments are shown. Fluorescence intensity of osteocalcin in cells on five random areas was measured with the microscope software (B) (FV10-ASW, Olympus). Significant differences versus cells on untreated titanium are shown as $*p < 0.05$.

expression of the osteogenic promoter WNT and its cell surface receptor Frizzled. Furthermore, NaOH treatment induced expression of Axin and adenomatous polyposis coli (APC), scaffold proteins that bind to intracellular Wnt/β-catenin signaling molecules. The receptor activator of nuclear factor-kappaB ligand (RANKL) decoy receptor osteoprotegerin (OPG) was upregulated by NaOH treatment (Fig. 5). $CaCl_2$ treatment induced expression of Frizzled, Axin, APC, and osteogenic markers BMP and IGF-1. Bone matrix protein OPN expression was upregulated by $CaCl_2$ treatment. Expression of integrin β3 was also induced following OPN upregulation by $CaCl_2$ (Fig. 6). $Ca(OH)_2$ treatment induced LRP5/6 and essential coreceptors of Wnt ligands for canonical β-catenin-dependent signal transduction, in addition to WNT, Frizzled, Axin, and APC. RANKL, which functions as a key factor for osteoclast differentiation and activation, was induced by $Ca(OH)_2$, in addition to BMP, IGF-1, and integrin β3. OCN expression was also upregulated by $Ca(OH)_2$ (Fig. 7).

DISCUSSION

The surface characteristics and chemical composition of titanium are critical in determining biocompatibility. The topography of titanium affects protein adsorption[1,2] and cell–material interactions and regulates osteointegration.[12,23,24,37,38] In this study, we evaluated the influence of chemically modified titanium surface topography on the incorporation of calcium ions on osteogenic differentiation in hMSCs. Sodium hydrogen titanate is formed on the titanium surface by alkali (NaOH) treatment; subsequently, apatite formation is initiated on the chemically treated surface when it is soaked in simulated body fluid.[18,19] Apatite formation is slightly improved on titanium surfaces treated with $CaCl_2$ after NaOH treatment to incorporate calcium ions into the surface.[26] Therefore, we focused on calcium ion incorporation into the titanium surface and investigated the influence of that modification on hMSC differentiation toward an

TABLE I. Significantly Upregulated Genes in Cells Grown on NaOH-Treated Titanium Disks (Top 30)

Symbol	Entrez Gene Name	Fold Change
TFPI2	Tissue factor pathway inhibitor 2	4.990
PTGS1	Prostaglandin-endoperoxide synthase 1 (prostaglandin G/H synthase and cyclooxygenase)	4.821
CXCL6	Chemokine (C-X-C motif) ligand 6 (granulocyte chemotactic protein 2)	4.387
PRSS1/PRSS3	Protease, serine, 1 (trypsin 1)	4.290
SERPINB2	Serpin peptidase inhibitor, clade B (ovalbumin), member 2	3.989
IL6R	Interleukin 6 receptor	3.612
PAPPA	Pregnancy-associated plasma protein A, pappalysin 1	3.434
AOX1	Aldehyde oxidase 1	3.223
CSGALNACT 1	Chondroitin sulfate N-acetylgalactosaminyltransferase 1	3.197
YTHDC1	YTH domain containing 1	3.169
GPR56	G protein-coupled receptor 56	3.155
OASL	2′-5′-Oligoadenylate synthetase-like	3.091
C10orf18	Family with sequence similarity 208, member B	3.056
ITGB1	Integrin, beta 1 (fibronectin receptor, beta polypeptide, antigen CD29 includes MDF2, MSK12)	2.996
HIST1H2BD	Histone cluster 1, H2bd	2.992
GALNTL2	UDP-N-acetyl-alpha-D-galactosamine:polypeptide N-Acetylgalactosaminyltransferase-like 2	2.911
IL17RC	Interleukin 17 receptor C	2.892
TNFSF13B	Tumor necrosis factor (ligand) superfamily, member 13b	2.736
FAM65B	Family with sequence similarity 65, member B	2.655
RIN3	Ras and Rab interactor 3	2.653
CCL2	Chemokine (C-C motif) ligand 2	2.647
FRAT1	Frequently rearranged in advanced T-cell lymphomas	2.645
CENPM	Centromere protein M	2.634
TPD52	Tumor protein D52	2.624
TNFSF15	Tumor necrosis factor (ligand) superfamily, member 15	2.597
SFTPA2	Surfactant protein A2	2.574
NR4A2	Nuclear receptor subfamily 4, group A, member 2	2.571
IFI6	Interferon, alpha-inducible protein 6	2.567
SMCHD1	Structural maintenance of chromosomes flexible hinge domain containing 1	2.541
PLCL2	Phospholipase C-like 2	2.488

osteogenic lineage. We also compared calcium ion modification by $CaCl_2$ and $Ca(OH)_2$.

Experimental titanium disks were treated with aqueous NaOH, $CaCl_2$, and $Ca(OH)_2$ solutions. hMSC morphology was altered and proliferation was significantly reduced by calcium surface treatment of titanium disks [Fig. 2(A,B)]. Several studies have demonstrated a link between cell shape and osteogenic differentiation in hMSCs.[39–42] In addition, incorporation of calcium ions and apatite formation on the titanium surface treated with $Ca(OH)_2$ were significantly greater than on $CaCl_2$-treated titanium disks [Fig. 1(B,C)]. To investigate the osteogenic differentiation of hMSCs cultured on chemically modified titanium disks, the expression of structural genes for the bone matrix OPN and the marker of bone formation OCN and OCN protein expression were examined (Figs. 3 and 4). OPN transcription in hMSCs was significantly upregulated by the calcium surface treatment, and was significantly on $Ca(OH)_2$-treated disks than on $CaCl_2$-treated disks. OCN protein expression was also upregulated by $Ca(OH)_2$ treatment; however, $CaCl_2$ treatment had no effect on the transcript and protein expression of OCN. We conclude that calcium surface treatment of the titanium disks influenced the osteogenic differentiation of hMSCs, and $Ca(OH)_2$ treatment of the titanium surface induced osteogenic differentiation, whereas $CaCl_2$ treatment had a limited effect.

To investigate the mechanism of osteogenic induction in hMSCs by calcium ions, comparative gene expression profiles were assessed by DNA microarray and pathway analyses. Several genes involved in osteogenic differentiation and bone metabolism were significantly upregulated by the chemical modifications of titanium. IL6R and ITGB1 were significantly upregulated by NaOH (Table I). SPP1 (OPN), MMP13, and ENPP1 were significantly upregulated by $CaCl_2$ and $Ca(OH)_2$ (Tables II and III). $Ca(OH)_2$ treatment also significantly upregulated the expression of IL6R, ITGA2, BMP2, and PTHLH (Table III). In addition, to differentiate the effect of two kinds of calcium surface treatments on gene expression, we compared $CaCl_2$ and $Ca(OH)_2$ treatments and found that $Ca(OH)_2$ treatment significantly upregulated expression of BMP2, PTGS2 (Cox2), PTHLH, and SPP1 (OPN) in hMSCs (Table IV). Previous studies have demonstrated Cox2 function is essential for bone formation in rats[43] and osteoblast differentiation is stimulated through induction of Cox2 in

TABLE II. Significantly Upregulated Genes in Cells Grown on $CaCl_2$-Treated Titanium Disks (Top 30)

Symbol	Entrez Gene Name	Fold Change
SPP1 (OPN)	Secreted phosphoprotein 1	6.252
PRSS1/PRSS3	Protease, serine, 1 (trypsin 1)	4.009
MMP13	Matrix metallopeptidase 13 (collagenase 3)	3.882
GPR56	G protein-coupled receptor 56	3.640
C13orf15	Regulator of cell cycle	3.578
IGFBP1	Insulin-like growth factor binding protein 1	3.540
PTGS1	Prostaglandin-endoperoxide synthase 1 (prostaglandin G/H synthase and cyclooxygenase)	3.500
TFPI2	Tissue factor pathway inhibitor 2	3.406
YTHDC1	YTH domain containing 1	3.371
CENPM	Centromere protein M	3.235
COL15A1	Collagen, type XV, alpha 1	3.174
AQP1	Aquaporin 1 (Colton blood group)	3.149
RPL18A	Ribosomal protein L18a	3.098
DUSP4	Dual specificity phosphatase 4	3.095
DIXDC1	DIX domain containing 1	3.016
TMEM158	Transmembrane protein 158 (gene/pseudogene)	2.791
C16orf57	Chromosome 16 open reading frame 57	2.787
SMC1A	Structural maintenance of chromosomes 1A	2.761
ARID5B	AT rich interactive domain 5B (MRF1-like)	2.655
TNFSF10	Tumor necrosis factor (ligand) superfamily, member 10	2.648
IL17RC	Interleukin 17 receptor C	2.624
DCTN4	Dynactin 4 (p62)	2.605
ING3	Inhibitor of growth family, member 3	2.557
NOL6	Nucleolar protein family 6 (RNA-associated)	2.555
PLTP	Phospholipid transfer protein	2.555
SLC29A1	Solute carrier family 29 (nucleoside transporters), member 1	2.507
MCM5	Minichromosome maintenance complex component 5	2.502
ENPP1	Ectonucleotide pyrophosphatase/phosphodiesterase 1	2.497
ADAMTS16	ADAM metallopeptidase with thrombospondin type 1 motif, 16	2.493
SMURF1	SMAD specific E3 ubiquitin protein ligase 1	2.491

TABLE III. Significantly Upregulated Genes in Cells Grown on $Ca(OH)_2$-Treated Titanium Disks (Top 30)

Symbol	Entrez Gene Name	Fold Change
SPP1 (OPN)	Secreted phosphoprotein 1	17.721
MMP13	Matrix metallopeptidase 13 (collagenase 3)	16.725
RGS2	Regulator of G-protein signaling 2, 24kDa	8.677
TFPI2	Tissue factor pathway inhibitor 2	7.763
PTGS1	Prostaglandin-endoperoxide synthase 1 (prostaglandin G/H synthase and cyclooxygenase)	7.343
SLC16A6	Solute carrier family 16, member 6 (monocarboxylic acid transporter 7)	7.286
IGFBP1	Insulin-like growth factor binding protein 1	6.677
DUSP4	Dual specificity phosphatase 4	6.649
PCDH19	Protocadherin 19	5.943
PTHLH	Parathyroid hormone-like hormone	5.630
GPR56	G protein-coupled receptor 56	5.129
SLC29A1	Solute carrier family 29 (nucleoside transporters), member 1	4.924
C13orf15	Regulator of cell cycle	4.750
ENPP1	Ectonucleotide pyrophosphatase/phosphodiesterase 1	4.717
EREG	Epiregulin	4.712
TNFSF10	Tumor necrosis factor (ligand) superfamily, member 10	4.436
CXCL6	Chemokine (C-X-C motif) ligand 6 (granulocyte chemotactic protein 2)	4.404
TMEM158	Transmembrane protein 158 (gene/pseudogene)	4.403
PRSS1/PRSS3	Protease, serine, 1 (trypsin 1)	4.397
BMP2	Bone morphogenetic protein 2	4.140
COL10A1	Collagen, type X, alpha 1	3.739
FOXQ1	Forkhead box Q1	3.670
MGP	Matrix Gla protein	3.488
PLAU	Plasminogen activator, urokinase	3.364
CENPM	Centromere protein M	3.288
IL6R	Interleukin 6 receptor	3.223
ITGA2	Integrin, alpha 2 (CD49B, alpha 2 subunit of VLA-2 receptor)	3.205
CLU	Clusterin	3.163
FPR1	Formyl peptide receptor 1	3.114
ESCO2	Establishment of cohesion 1 homolog 2 (*S. cerevisiae*)	3.084

TABLE IV. Significantly Upregulated Genes Associated with 'Formation of Bone' on $Ca(OH)_2$-Treated Titanium Disks vs. $CaCl_2$-Trated Disks

Symbol	Entrez Gene Name	Fold Change
SPP1 (OPN)	Secreted phosphoprotein 1 (Osteopontin)	2.835
PTHLH	Parathyroid hormone-like hormone	2.308
FGF1	Fibroblast growth factor 1 (acidic)	2.202
BMP2	Bone morphogenetic protein 2	2.175
PTGS1	Prostaglandin-endoperoxide synthase 1 (prostaglandin G/H synthase and cyclooxygenase 1)	2.098
PTGS2	Prostaglandin-endoperoxide synthase 2 (prostaglandin G/H synthase and cyclooxygenase 2)	2.008

These genes significantly overlapped with the genes associated with "formation of bone" by IPA ($p = 3.96 \times 10^{-4}$).

mesenchymal progenitor cells.[44] BMP2 induces Cox2 in osteoblasts[45] and in mesenchymal cells.[46] It was also reported that extracellular calcium increases expression of BMP2.[47,48] Furthermore, the calcium–calcineurin–nuclear factor of activated T-cell signaling pathway has an important role in the PTH induction of Cox2.[49] Taken together, our results suggest that $Ca(OH)_2$ treatment of titanium disks induces osteogenic differentiation in hMSCs via induction of BMP2, Cox2, and PTHLH. In contrast, Smad signaling was downregulated by chemically modified titanium surfaces (Figs. 5–7). A previous study demonstrated that noncanonical BMP signaling regulates Cox2 transcription.[46] These observations suggest noncanonical BMP signaling (independent of Smad signaling) might mediate the osteogenic differentiation of hMSCs on $Ca(OH)_2$-treated titanium.

Postanalysis of microarray data was performed by IPA. NaOH treatment induced the osteogenic promoter WNT and its cell surface receptor Frizzled, as well as Axin and APC,

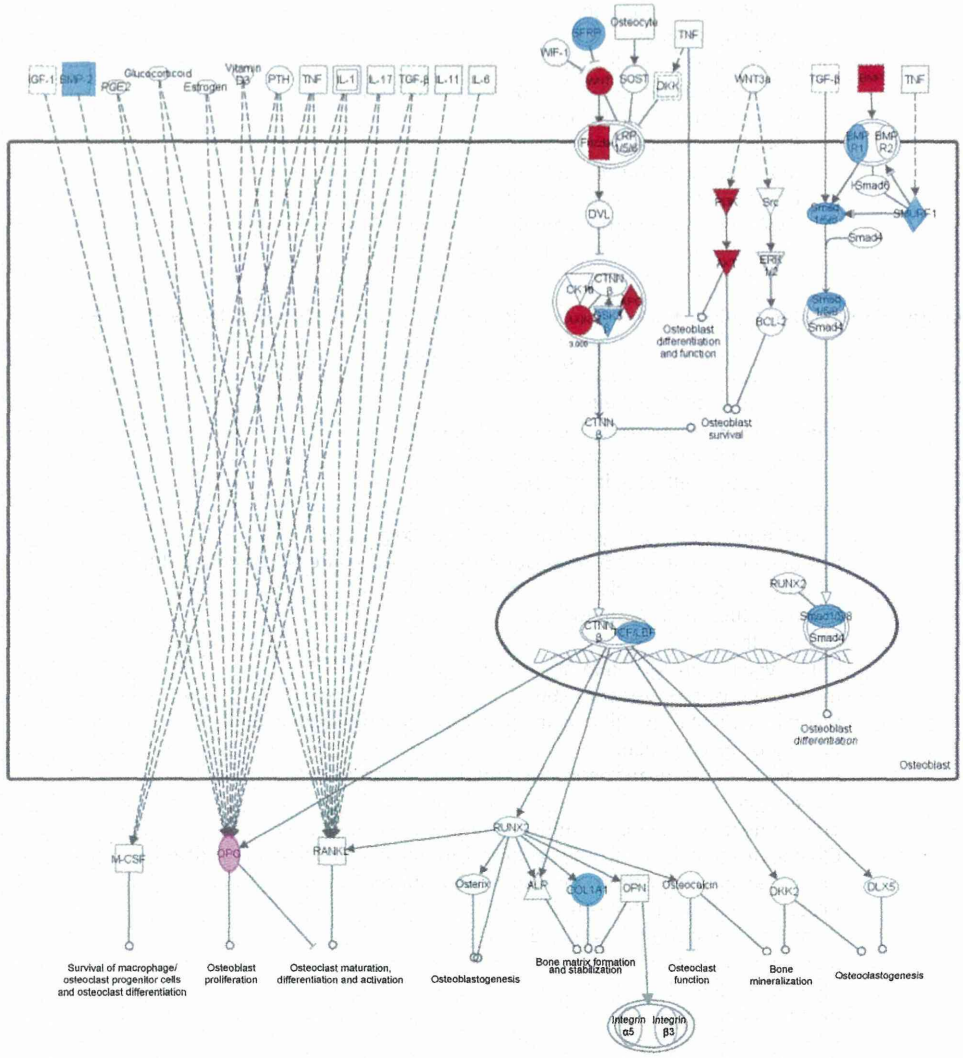

FIGURE 5. Differentially expressed genes in the canonical pathway in osteoblasts were significantly changed by NaOH treatment versus untreated conditions. Upregulated (more than twice), downregulated (less than 1/2), induced, and suppressed genes are indicated in pink, green, red, and light blue, respectively.

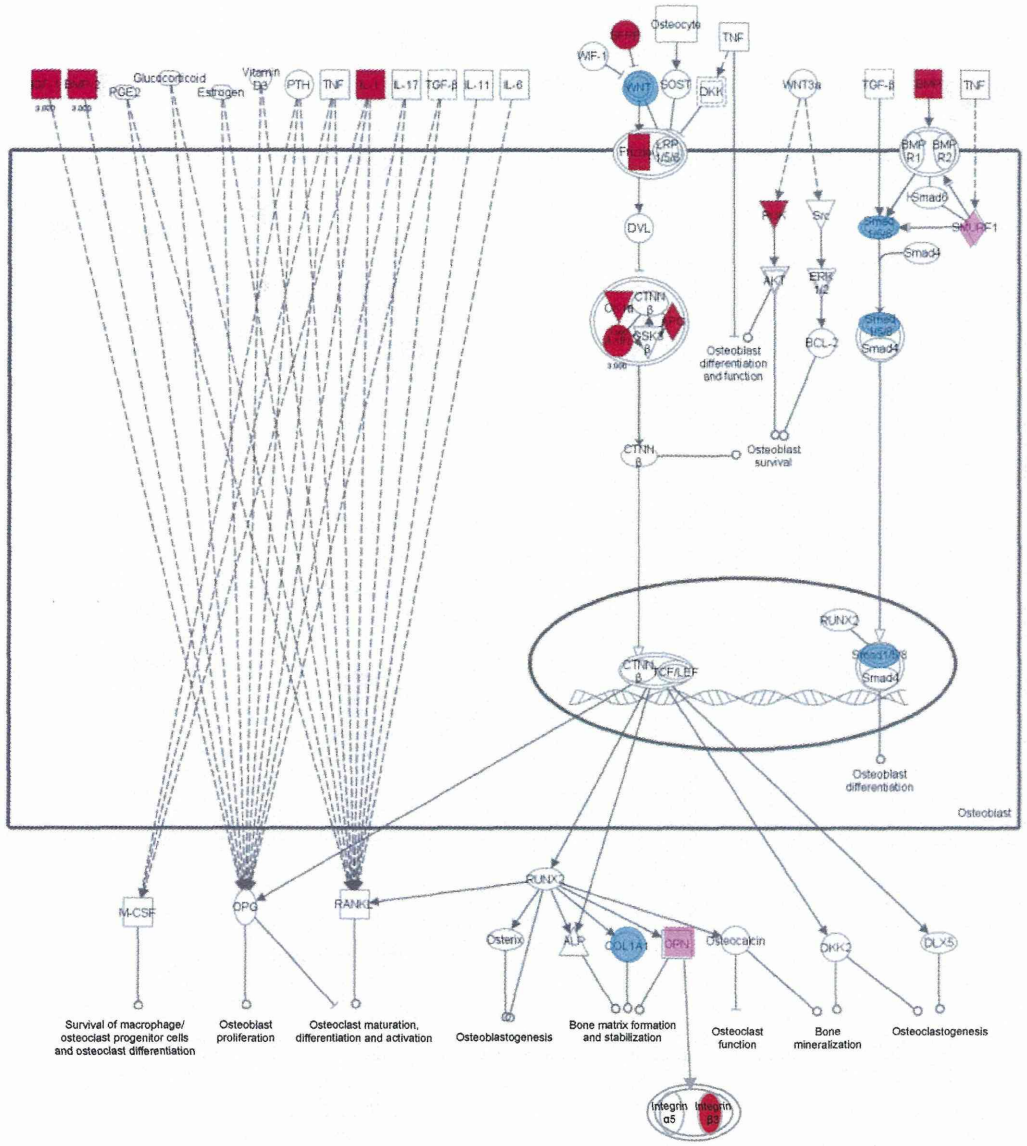

FIGURE 6. Differentially expressed genes in the canonical osteoblast pathway on $CaCl_2$-treated disks versus untreated disks. Upregulated (more than twice), downregulated (less than 1/2), induced, and suppressed genes are indicated in pink, green, red, and light blue, respectively.

scaffolding proteins that bind to intracellular Wnt/β-catenin signaling molecules. RANKL decoy receptor OPG expression was upregulated by NaOH (Fig. 5). $CaCl_2$ treatment induced expression of Frizzled, Axin, and APC as well as of the osteogenic markers BMP and IGF-1. The bone matrix protein OPN was upregulated, and the expression of integrin β3 was induced following OPN upregulation by $CaCl_2$ (Fig. 6). $Ca(OH)_2$ treatment induced LRP5/6 and essential coreceptors of Wnt ligands for canonical β-catenin-dependent signal transduction, in addition to WNT, Frizzled, Axin, and APC. BMP, IGF-1, and integrin β3 were also induced by $Ca(OH)_2$. In addition to OPN, OCN was upregulated by $Ca(OH)_2$ (Fig. 7).

Wnt/β-catenin signaling in mesenchymal progenitors controls osteoblast differentiation[50]; surface properties of titanium regulate stem cell fate and induce osteoblast differentiation via the Wnt calcium-dependent pathway and Wnt5a enhanced osteogenesis through positive feedback with integrins.[51] Previous studies have shown the integrin family plays a major role in osteoblastic differentiation on variously modified titanium surfaces.[4,5,10,14] We observed that calcium modification of the titanium surface induced integrin β3 following OPN upregulation. Wnt/β-catenin signaling in hMSCs was also promoted by the calcium modification, more by $Ca(OH)_2$ than $CaCl_2$ treatment. These observations suggest that calcium modification of titanium surfaces induces osteogenic differentiation in hMSCs in the absence of osteogenic factors by activation of Wnt/β-catenin signaling.

In this study, $Ca(OH)_2$ treatment of titanium surface was more effective to osteogenic differentiation in hMSC than $CaCl_2$ treatment, this might be caused by the difference of the amount of calcium ions and apatite formation on the titanium surface between the two kinds of calcium treatments. We

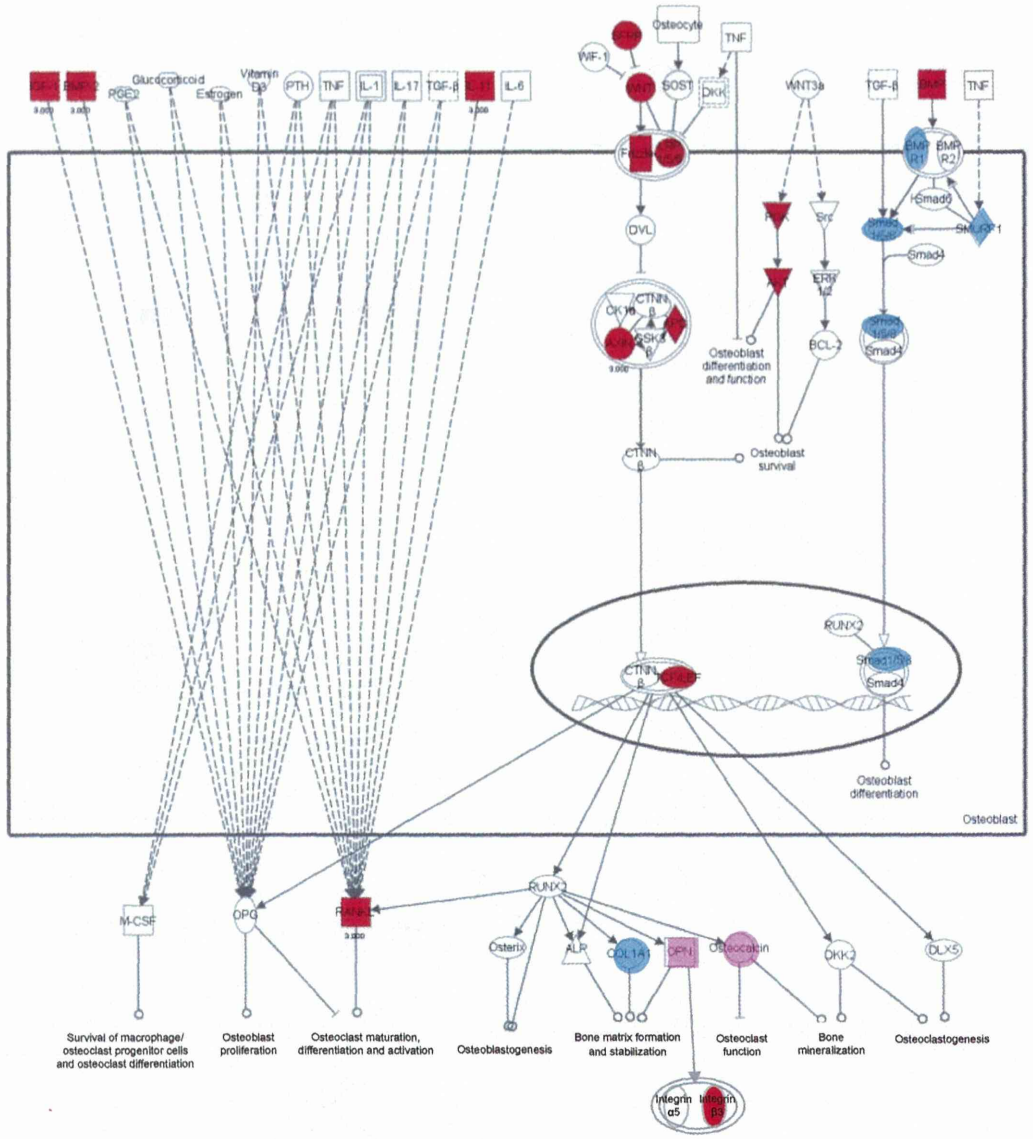

FIGURE 7. Differentially expressed genes in the canonical osteoblast pathway on $Ca(OH)_2$ versus untreated disks. Upregulated (more than twice), downregulated (less than 1/2), induced, and suppressed genes are indicated in pink, green, red, and light blue, respectively.

suggested that $Ca(OH)_2$ treatment of titanium disks induced osteogenic differentiation in hMSCs by the upregulation of BMP2, Cox2, and PTHLH compared with $CaCl_2$ treatment, and the activation of Wnt/β-catenin signaling.

CONCLUSIONS

In this study, we chemically modified titanium surfaces with $CaCl_2$ or $Ca(OH)_2$ after NaOH treatment to alter the surface topology and incorporate calcium ions; subsequently, we investigated the influence of these treatments on osteogenic differentiation in hMSCs in the absence of osteogenic supplements. Calcium modification by $CaCl_2$ or $Ca(OH)_2$ affects cell morphology and molecular responses in hMSCs. Whole genome expression analysis suggested that calcium modification of the titanium surface activates Wnt/β-catenin signaling. In addition, $Ca(OH)_2$ treatment upregulated expression of BMP2, Cox2, and PTHLH. $Ca(OH)_2$ treatment induces osteogenic differentiation in hMSCs, whereas $CaCl_2$ has a limited effect; this may depend on whether there are significant differences between treatments with respect to the amount of calcium ions and apatite formation on the titanium surface.

ACKNOWLEDGMENTS

This work was supported by the Health and Labour Sciences Research Grants for Research on Regulatory Science of Pharmaceuticals and Medical Devices (H22-IYAKU-IPPAN-009, H24- IYAKU-SHITEI-018) from the Ministry of Health, Labour and Welfare of Japan.

REFERENCES

1. Walivaara B, Aronsson BO, Rodahl M, Lausmaa J, Tengvall P. Titanium with different oxides: In vitro studies of protein adsorption and contact activation. Biomaterials 1994;15:827–834.

2. Rupp F, Axmann D, Ziegler C, Geis-Gerstorfer J. Adsorption/desorption phenomena on pure and Teflon AF-coated titania surfaces studied by dynamic contact angle analysis. J Biomed Mater Res 2002;62:567–578.
3. Sousa SR, Lamghari M, Sampaio P, Moradas-Ferreira P, Barbosa MA. Osteoblast adhesion and morphology on TiO_2 depends on the competitive preadsorption of albumin and fibronectin. J Biomed Mater Res A 2008;84:281–290.
4. Anselme K. Osteoblast adhesion on biomaterials. Biomaterials 2000;21:667–681.
5. Lavenus S, Berreur M, Trichet V, Pilet P, Louarn G, Layrolle P. Adhesion and osteogenic differentiation of human mesenchymal stem cells on titanium nanopores. Eur Cell Mater 2011;22:84–96; discussion 96.
6. Hu Y, Cai K, Luo Z, Zhang Y, Li L, Lai M, Hou Y, Huang Y, Li J, Ding X, Zhang B, Sung KL. Regulation of the differentiation of mesenchymal stem cells in vitro and osteogenesis in vivo by microenvironmental modification of titanium alloy surfaces. Biomaterials 2012;33:3515–3528.
7. Vlacic-Zischke J, Hamlet SM, Friis T, Tonetti MS, Ivanovski S. The influence of surface microroughness and hydrophilicity of titanium on the up-regulation of TGFbeta/BMP signalling in osteoblasts. Biomaterials 2011;32:665–671.
8. Khang D, Choi J, Im YM, Kim YJ, Jang JH, Kang SS, Nam TH, Song J, Park JW. Role of subnano-, nano- and submicron-surface features on osteoblast differentiation of bone marrow mesenchymal stem cells. Biomaterials 2012;33:5997–6007.
9. Gittens RA, McLachlan T, Olivares-Navarrete R, Cai Y, Berner S, Tannenbaum R, Schwartz Z, Sandhage KH, Boyan BD. The effects of combined micron-/submicron-scale surface roughness and nanoscale features on cell proliferation and differentiation. Biomaterials 2011;32:3395–3403.
10. Olivares-Navarrete R, Raz P, Zhao G, Chen J, Wieland M, Cochran DL, Chaudhri RA, Ornoy A, Boyan BD, Schwartz Z. Integrin alpha2beta1 plays a critical role in osteoblast response to micron-scale surface structure and surface energy of titanium substrates. Proc Natl Acad Sci USA 2008;105:15767–15772.
11. Wennerberg A, Albrektsson T. Effects of titanium surface topography on bone integration: A systematic review. Clin Oral Implants Res 2009;20(Suppl 4):172–184.
12. Schwartz Z, Nasazky E, Boyan BD. Surface microtopography regulates osteointegration: The role of implant surface microtopography in osteointegration. Alpha Omegan 2005;98:9–19.
13. Park JH, Olivares-Navarrete R, Wasilewski CE, Boyan BD, Tannenbaum R, Schwartz Z. Use of polyelectrolyte thin films to modulate osteoblast response to microstructured titanium surfaces. Biomaterials 2012;33:5267–5277.
14. Wang L, Zhao G, Olivares-Navarrete R, Bell BF, Wieland M, Cochran DL, Schwartz Z, Boyan BD. Integrin beta1 silencing in osteoblasts alters substrate-dependent responses to 1,25-dihydroxy vitamin D3. Biomaterials 2006;27:3716–3725.
15. Guo J, Padilla RJ, Ambrose W, De Kok IJ, Cooper LF. The effect of hydrofluoric acid treatment of TiO2 grit blasted titanium implants on adherent osteoblast gene expression in vitro and in vivo. Biomaterials 2007;28:5418–5425.
16. Mendonca G, Mendonca DB, Simoes LG, Araujo AL, Leite ER, Duarte WR, Aragao FJ, Cooper LF. The effects of implant surface nanoscale features on osteoblast-specific gene expression. Biomaterials 2009;30:4053–4062.
17. Mendonca G, Mendonca DB, Aragao FJ, Cooper LF. The combination of micron and nanotopography by H_2SO_4/H_2O_2 treatment and its effects on osteoblast-specific gene expression of hMSCs. J Biomed Mater Res A 2010;94:169–179.
18. Kim HM, Miyaji F, Kokubo T, Nakamura T. Preparation of bioactive Ti and its alloys via simple chemical surface treatment. J Biomed Mater Res 1996;32:409–417.
19. Yan WQ, Nakamura T, Kobayashi M, Kim HM, Miyaji F, Kokubo T. Bonding of chemically treated titanium implants to bone. J Biomed Mater Res 1997;37:267–275.
20. Kim HM, Miyaji F, Kokubo T, Nishiguchi S, Nakamura T. Graded surface structure of bioactive titanium prepared by chemical treatment. J Biomed Mater Res 1999;45:100–107.
21. Takadama H, Kim HM, Kokubo T, Nakamura T. TEM-EDX study of mechanism of bonelike apatite formation on bioactive titanium metal in simulated body fluid. J Biomed Mater Res 2001;57:441–448.
22. Nishiguchi S, Kato H, Neo M, Oka M, Kim HM, Kokubo T, Nakamura T. Alkali- and heat-treated porous titanium for orthopedic implants. J Biomed Mater Res 2001;54:198–208.
23. Fujibayashi S, Neo M, Kim HM, Kokubo T, Nakamura T. Osteoinduction of porous bioactive titanium metal. Biomaterials 2004;25:443–450.
24. Takemoto M, Fujibayashi S, Neo M, Suzuki J, Kokubo T, Nakamura T. Mechanical properties and osteoconductivity of porous bioactive titanium. Biomaterials 2005;26:6014–6023.
25. Cooper LF, Zhou Y, Takebe J, Guo J, Abron A, Holmen A, Ellingsen JE. Fluoride modification effects on osteoblast behavior and bone formation at TiO2 grit-blasted c.p. titanium endosseous implants. Biomaterials 2006;27:926–936.
26. Kizuki T, Takadama H, Matsushita T, Nakamura T, Kokubo T. Preparation of bioactive Ti metal surface enriched with calcium ions by chemical treatment. Acta Biomater 2010;6:2836–2842.
27. Jiang Y, Jahagirdar BN, Reinhardt RL, Schwartz RE, Keene CD, Ortiz-Gonzalez XR, Reyes M, Lenvik T, Lund T, Blackstad M, Du J, Aldrich S, Lisberg A, Low WC, Largaespada DA, Verfaillie CM. Pluripotency of mesenchymal stem cells derived from adult marrow. Nature 2002;418:41–49.
28. Rosenthal N. Prometheus's vulture and the stem-cell promise. N Engl J Med 2003;349:267–274.
29. Korbling M, Estrov Z. Adult stem cells for tissue repair—A new therapeutic concept? N Engl J Med 2003;349:570–582.
30. Hishikawa K, Miura S, Marumo T, Yoshioka H, Mori Y, Takato T, Fujita T. Gene expression profile of human mesenchymal stem cells during osteogenesis in three-dimensional thermoreversible gelation polymer. Biochem Biophys Res Commun 2004;317:1103–1107.
31. Horwitz EM, Gordon PL, Koo WK, Marx JC, Neel MD, McNall RY, Muul L, Hofmann T. Isolated allogeneic bone marrow-derived mesenchymal cells engraft and stimulate growth in children with osteogenesis imperfecta: Implications for cell therapy of bone. Proc Natl Acad Sci USA 2002;99:8932–8937.
32. Mangi AA, Noiseux N, Kong D, He H, Rezvani M, Ingwall JS, Dzau VJ. Mesenchymal stem cells modified with Akt prevent remodeling and restore performance of infarcted hearts. Nat Med 2003;9:1195–1201.
33. Strauer BE, Brehm M, Zeus T, Kostering M, Hernandez A, Sorg RV, Kogler G, Wernet P. Repair of infarcted myocardium by autologous intracoronary mononuclear bone marrow cell transplantation in humans. Circulation 2002;106:1913–1918.
34. Petersen BE, Bowen WC, Patrene KD, Mars WM, Sullivan AK, Murase N, Boggs SS, Greenberger JS, Goff JP. Bone marrow as a potential source of hepatic oval cells. Science 1999;284:1168–1170.
35. Behonick DJ, Xing Z, Lieu S, Buckley JM, Lotz JC, Marcucio RS, Werb Z, Miclau T, Colnot C. Role of matrix metalloproteinase 13 in both endochondral and intramembranous ossification during skeletal regeneration. PLoS One 2007;2:e1150.
36. Dvorak-Ewell MM, Chen TH, Liang N, Garvey C, Liu B, Tu C, Chang W, Bikle DD, Shoback DM. Osteoblast extracellular Ca^{2+}-sensing receptor regulates bone development, mineralization, and turnover. J Bone Miner Res 2011;26:2935–2947.
37. Albrektsson T, Wennerberg A. Oral implant surfaces: Part 1—Review focusing on topographic and chemical properties of different surfaces and in vivo responses to them. Int J Prosthodont 2004;17:536–543.
38. Albrektsson T, Wennerberg A. Oral implant surfaces: Part 2—Review focusing on clinical knowledge of different surfaces. Int J Prosthodont 2004;17:544–564.
39. McBeath R, Pirone DM, Nelson CM, Bhadriraju K, Chen CS. Cell shape, cytoskeletal tension, and RhoA regulate stem cell lineage commitment. Dev Cell 2004;6:483–495.
40. Rodriguez JP, Gonzalez M, Rios S, Cambiazo V. Cytoskeletal organization of human mesenchymal stem cells (MSC) changes during their osteogenic differentiation. J Cell Biochem 2004;93:721–731.
41. Kumar G, Tison CK, Chatterjee K, Pine PS, McDaniel JH, Salit ML, Young MF, Simon CG Jr. The determination of stem cell fate by 3D scaffold structures through the control of cell shape. Biomaterials 2011;32:9188–9196.